Climate Change, Food Prices, and Inequality*

Mauricio Barbosa-Alves **Braulio Britos**

Job Market Paper

University of Minnesota *University of Minnesota*

November 12, 2024

Regularly updated; click here for the most recent version

Abstract

This paper analyzes the impact of climate change on food prices across regions and income groups, focusing on how uneven agricultural productivity affects inequality. As climate change shifts comparative advantages in food production, trade frictions limit adaptive sourcing. Poor households, with higher food expenditure shares, are particularly vulnerable to local price increases. In particular, local productivity is the key determinant of the relative price of food goods that face high trade costs. We develop a spatial macro trade model that incorporates income heterogeneity and two types of food goods with different trade frictions, allowing us to decompose welfare losses into food expenditure shares, trade shares, and productivity changes. Using Brazilian data, we estimate intra-national trade shares through short-term weather shocks, price changes, and driving times between states. The results show that trade frictions for fresh food are twice as sensitive to driving time compared to commodities. Counterfactuals based on productivity forecasts indicate substantial welfare losses, with the lowest income decile in the most affected states willing to forgo 3% of income to avoid projected productivity declines. Improving road infrastructure could mitigate these effects, with low-income households willing to pay up to 0.8% of income for a 10% increase in average driving speed.

JEL classification: E31, F16, O44, Q54, Q56.

Keywords: Climate Change, Trade Frictions, Food Prices, Inequality, Agricultural Productivity

*Mauricio Barbosa-Alves: barbo104@umn.edu. Braulio Britos: gb.britosh@gmail.com. We thank our advisors, Manuel Amador and Tim Kehoe, and Doireann Fitzgerald, for their invaluable guidance during this project. We thank Ilenin Kondo, Joseph Mullins, Michael E. Waugh for their comments on several stages of this project. We thank Ricardo Alves Monteiro, Diego Ascarza Mendoza, Teresa Balestrini, Marco Bassetto, Hasan Cetin, Gabriel Devoto, Rene Diaz de Leon, Angelo Mendes, Jakub Pawelczak, and the participants in the Trade Workshop at the University of Minnesota, the Wisconsin-Minnesota Graduate Student Workshop, and the Minnesota Jamboree for their comments and suggestions. All errors are our own.

1 Introduction

Climate change is expected to reshape the spatial patterns of agricultural productivity. One adaptive strategy involves leveraging novel comparative advantages through the re-optimization of food sourcing. Nevertheless, due to the high costs associated with transporting goods over distances, trade barriers restrict the degree to which this process can happen. For items that incur substantial transportation costs, the significance of local productivity becomes paramount. With the rise in food prices, the welfare implications are not uniformly distributed across various income levels, as lower-income households usually spend a higher proportion of their budget on food.

What effects will climate change have on food prices and how will it influence individuals across various income levels? To address this question, we develop a spatial model of food production and trade, building on Eaton and Kortum (2002) and Costinot et al. (2016). Our model incorporates rich heterogeneity in four dimensions. First, to examine the importance of trade ease, we distinguish between two types of food goods, each facing different trade costs. Second, locations vary in productivity for each type of food. Third, locations are distinct regarding their degree of connectedness to others. Fourth, income levels within each location vary, with both relatively richer and poorer households.

In our model, locations produce goods based on their productivity and engage in trade. Food goods face varying trade costs, which distort the comparative advantages of locations and influence trade patterns. Goods with higher trade costs exhibit a greater spatial price dispersion compared to those with lower trade costs. For high-trade-cost goods, local productivity is especially critical, as lower productivity leads to higher prices.

We calculate the welfare effects stemming from changes in food prices. In our setting, shifts in utility caused by climate change are driven solely by changes in food prices, as household income is constant. We decompose the equivalent variation from climate change into three components, drawing on standard demand theory. The first is the food expenditure share: poorer households, with higher food expenditure shares, are more sensitive to changes in food prices. The second is the trade shares between locations, which reflect how regions are affected by productivity changes in other regions they trade with, including themselves. The third component captures changes in potential food productivity across different areas.

We apply the model to Brazil, treating each state as a separate location. Given Brazil's vast latitude range and tropical climate, there are significant productivity differences across regions and crops. The country's extensive land coverage and reliance on road-based transportation make the movement of goods challenging. Additionally, income inequality is pronounced both within and across states.

Trade flows and frictions are central to our model, but not directly observed in the data. This is a frequently encountered issue in domestic trade is the necessity for comprehensive information on trade flows among sub-national units, hardly observed in the data. As in many studies of intra-national trade, e.g, Ramondo et al. (2016), Pellegrina (2022), Sotelo (2020), the trade flows are not directly observable in data between Brazilian states[1]. To overcome this data constraint, we incorporate the model structure with the inclusion of short-term weather variances, allowing us to derive a correlation between price fluctuations and weather anomalies, both quantifiable in the data. We then employ this observed variation in prices and weather disturbances to extract estimates of these trade barriers for different types of food goods.

In our model, heat shocks reduce food productivity, driving up prices. Neighboring states are also affected, as they import food from the impacted state. Thus, the observed price change in any state reflects a weighted average of heat shocks between states, with the weights determined by trade shares. These shares depend on average potential productivity, labor costs, and bilateral trade frictions. To capture this structure, we combine a panel of Consumer Price Index (CPI) data with a panel of heat shocks. Drawing from crop science literature, e.g. Schlenker and Roberts, 2009, we focus on a temperature threshold of 30°C/86°F, known to harm crop yields. Using satellite weather data Copernicus Climate Change Service (2019), we construct a panel tracking the number of hours (in days) that temperatures exceeded this threshold in each city. We leverage these heat shocks to estimate trade frictions from variations in prices and temperatures and validate the threshold by showing evidence of yield declines when crops are exposed to such temperatures during the growing season.

To the extent that most cargo transportation within Brazil rely on trucks via roads (World

[1]This feature is common across most countries. Canada is a noticeable exception, which releases interprovincial trade flows. See, e.g., Agnosteva et al. (2014)

Bank, 2022), we model trade frictions as a function of driving time between states[2]. We build on a classification of food goods' tradability developed by the Brazilian Central Bank for tracking the CPI. Using this classification, we compute the price index for baskets of food products, in a panel of locations. One index includes goods that are frequently traded on the international market, such as commodities, while the other represents items that are less commonly traded globally, typically more perishable, fresh goods. We separately estimate the elasticity of trade costs with respect to the driving time for each basket. Our findings suggest that this elasticity is nearly double for goods with elevated trade costs, such as fresh goods, compared to those with reduced trade costs, such as commodities.

We examine how the spatial correlation of heat and price changes shape our results. While heat shocks naturally show positive spatial correlation, we document that a similar pattern for inflation dynamics across locations. Specifically, as driving time between locations increases, making them less connected, the inflation correlation decreases, especially for goods with higher trade costs. Our model capture this feature of the data: locations farther apart experience different heat shocks, and substantial trade frictions make local prices more dependent on nearby conditions. Thus, inflation correlations decline more sharply for high-trade-cost goods, with a more modest decline observed for low-trade-cost goods.

With these estimates of trade frictions and trade shares, we proceed to do counterfactual exercises. Actual production data often suffers from selection bias in Ricardian models, as locations tend to produce goods where they have a comparative advantage. Hence, the productivity across the spectrum of goods is latent: in the actual production data, we observe only partially these productivities. To address this, we use the *potential* productivity of crops across regions for each type of food good. Following our equivalent variation decomposition, we incorporate proportional changes in average potential productivity into the model. These estimates are sourced from the GAEZ project by FAO and IIASA (2022), based on various climate change scenarios.

The GAEZ project also provides data on the historical levels of this *potential* productivity. We employ this historical data for two reasons. First, it serves as an input to recover trade frictions. Second, it provides a benchmark to compare with alternative productivity forecasts from the GAEZ project. In our equivalent variation decomposition, changes in average potential productivity are

[2]World Bank (2022) shows data for 2021, with the estimated share of cargo transported by road is 66%. Railroads correspond to 18% and waterways other 15%.

central, making historical estimates a crucial basis for comparison.

The GAEZ project provides detailed data on agricultural productivity under various climate change scenarios, covering different time horizons and intensities of productivity shifts linked to greenhouse gas concentrations. Given the higher uncertainty over longer horizons, we focus our results using the optimistic scenario (RCP 2.6) for the period ending in 2040[3].

We show that even under the most optimistic climate change scenario, there is significant variation in potential productivity changes across states compared to historical baselines. Furthermore, there is substantial heterogeneity in the effect of climate change on productivity between food types, with high-trade-cost foods experiencing more pronounced declines in average potential productivity.

Using our equivalent variation analysis, we estimate how much households would be willing to pay to avoid the productivity changes linked to climate change. While food prices are an aggregate at the state level, within-state income heterogeneity leads to differentiated welfare effects of price increases. Due to non-homothetic preferences, food expenditure shares decline with income, consistent with observed data. Households in the lowest income decile are more vulnerable to changes in food prices, as they allocate a larger share of their income to food[4]. Under the optimistic scenario, households in the first income decile in some states would be willing to forgo up to 3% of their income to avoid these productivity shifts.

Finally, we argue that an effective adaptation strategy is to improve road quality. Since trade frictions are modeled as a function of driving time between states, increasing average road speed effectively reduces trade barriers. We derive a formula for the equivalent variation under this scenario, involving three components similar to the productivity change decomposition: food expenditure shares, trade shares between states, and the estimated elasticity of trade frictions with respect to driving time. We find that, given these elasticities, the sufficient statistic for the equivalent variation is the own trade share of each state, linking to findings from the international trade literature, (Arkolakis et al., 2012). For a 10% improvement in road quality, households in the lowest income decile would be willing to pay up to 0.8% of their income under the optimistic scenario.

[3]The GAEZ data employs four Representative Concentration Pathways (RCPs): 2.6, 4.5, 6.0, and 8.5 to construct scenarios. These values represent radiative forcing levels by 2100, reflecting greenhouse gas concentrations, with lower values indicating cooler temperatures and stricter mitigation policies.

[4]We show this pattern in figure 2.

Related Literature. Our paper intersects several branches of the literature. A central component of our analysis is the recovery of trade cost estimates, given the lack of detailed intra-national trade flow data. There is a growing body of work focused on identifying and measuring intra-national trade costs. Atkin and Donaldson (2015) summarizes the main challenges of the task. Some papers infer and bound trade costs using observed price differentials across locations, leveraging their model structures(Allen and Atkin, 2022; Donaldson and Hornbeck, 2016). Others papers (Donaldson, 2018), Asturias et al. (2019)) rely on the price differentials of some good produced by a monopolist or single factory to estimate trade costs, relating this dispersion to distance.

Sotelo (2020) uses price dispersion in coffee markets in Peru, together with road quality data, to measure trade frictions. Similarly to Donaldson (2018), the author assumes that trade friction is the same for all crops, depending only on the distance from the road. Focusing on Brazil, Pellegrina (2022) uses deviations in farm gate prices to estimate trade elasticities and the elasticity of trade costs with respect to driving time between locations. A related finding in this study is that the elasticity is twice as large for perishables relative to non-perishables, a result similar to ours, although we find a higher magnitude. Since we do not observe price levels, only changes in prices, we take a different approach to estimating trade frictions by using weather variability as a means to recover these estimates. Exploiting this link between weather shocks and prices changes is one of our contributions.

Our paper also contributes to the literature on the pass-through of shocks to prices. Auer et al. (2022) investigates the pass-through of the Swiss Franc's appreciation to consumer prices, while Fitzgerald (2008) examines how trade costs affect the pass-through from exchange rate movements to consumer prices. Faccia et al. (2021) uses a cross-country panel to assess the price dynamics of different consumption baskets after extreme weather events, such as sweltering summers or cold winters. We add to this literature by documenting increases in the local food prices following exposure to high temperatures, relying on detailed, disaggregate data for the temperatures.

We are also related to the literature on the economic effects of transitory weather shocks. Somanathan et al. (2021) documents declines in productivity and changes in labor supply in Indian factories exposed to high temperatures. Castro-Vincenzi et al. (2024) shows how firms diversify their sourcing across regions to mitigate the risk of floods in India. Oni (2024) investigates energy price variability and its disproportionate effects on low-income households' expenditure, studying

the distributional impact of energy price shocks. In Barbosa-Alves and Britos (2023), we studied how migration flows from rural Guatemala to the US are affected by local temperature shocks. Similar to our approach here, we use short-run fluctuations in temperature to inform about some frictions in the economy. We contribute to this literature by showing the usefulness of these transitory productivity shocks in the context of trade.

The growing literature on the economic impacts of climate change and potential mitigation and adaptation mechanisms is also relevant to our study. Costinot et al. (2016) analyzes agricultural adaptation to climate change on a global scale using an earlier version of the GAEZ data. Bilal and Känzig (2024) documents significant declines in global economic activity following a temperature shock. Bilal and Rossi-Hansberg (2023) incorporates a migration model to evaluate the impacts of climate change, utilizing damage assessments from natural events like storms and heatwaves. Cruz and Rossi-Hansberg (2024) estimates productivity and amenity losses due to rising temperatures, predicting welfare costs of up to 20% in Africa and Latin America. Our approach complements this literature by focusing on the intra-national level in Brazil, highlighting the role of food goods' tradability.

Our paper also examines the distributional effects of productivity changes. Fajgelbaum and Khandelwal (2016) measures unequal gains from trade based on variations in expenditure shares across the income distribution. The first-order approach employed in their study is also used in the counterfactual analysis by Costinot et al. (2016). Adao et al. (2017) develops a methodology for counterfactual analysis in trade models based on this first-order approach. We extend the discussion in Costinot et al. (2016) by focusing on the the heterogeneity of the expenditure shares and good (or type of) specific trade frictions at the intranational.

Outline. The remainder of the paper is organized as follows. Section 2 presents the trade component of the model. Section 3 derives a welfare change formula to highlight key elements for the counterfactual exercises. Section 4 introduces a perturbation to recover missing trade shares. Section 5 develops the demand side, specifying preferences and parameter calibration. Section 6 presents results from the counterfactuals, including the policy scenario on road infrastructure. Section 7 discuss limitations and potential extensions. The final section summarizes the findings.

2 Model

We develop a spatial model of food production and trade, incorporating heterogeneity along four dimensions: the tradability of different types of food, the productivity of each location for each food type, the degree of connectedness between locations, and income heterogeneity within each location.

The model includes three productive sectors: one referred to as the outside good sector, and two sectors producing different types of food, distinguished primarily by their degree of tradability. We classify the food sectors into two groups: one facing low trade costs and the other facing high trade costs. Each location is endowed with a distribution of potential productivities for goods of each type of food, and the outside good. Within each location, a population of households resides and supplies labor inelastically. These households do not migrate, and differ in their effective labor hours, generating income heterogeneity within each location.

Our approach proceeds as follows. First, we present the model without considering any shocks — either transitory shocks from weather or "permanent" shocks from climate change. As we develop the theoretical framework, we identify key missing data necessary for estimating the model, most notably detailed information on trade flows. We then introduce a transitory weather shock into the model and derive the link between price movements and the realization of these transitory shocks. This relationship is used to estimate trade frictions and recover trade shares. Finally, we discuss the sources of exogenous variation that underpin the counterfactual analysis.

2.1 The Trade Block

Our environment is static and there is no storage technology available. There are L locations, indexed by ℓ in the set $\mathcal{L} \equiv \{1, 2, \ldots, L\}$. A mass of households Λ_ℓ lives in location ℓ. Locations are endowed with productivity parameters, described momentarily.

Sectors, Goods, and Market Structure. There are three sectors: one producing an outside good, indexed by o, and sectors producing two types of food goods. One type faces low trade costs between regions, denoted by c, and another faces high trade costs, denoted by q. One might fix ideas by thinking of goods of type c as easily traded commodities, such as rice, soybean, corn, and

wheat, and think of goods indexed q as harder to trade or more perishables, such as tomatoes and lettuce. We denote $x \in \mathcal{X} \equiv \{c, q\}$ to ease the notation later. For each food type x, there is a unitary mass of goods, each indexed by $\omega \in [0, 1]$. We call a variety a pair of type and good (x, ω). In all that follows, we assume all markets are perfectly competitive so that prices are pinned down by the marginal production costs, on top of any transportation costs.

Transportation Costs. We model trade frictions as iceberg costs, and let the outside good o be traded without friction. As a result, the price of the outside good is the same across locations and, therefore, is well suited to serve as the numeraire.

For food products, all varieties of a given type x face a trade cost $\tau^x_{j,\ell}$ for the location pairs (j, ℓ) and the good type $x \in \{c, q\}$. As usual, the interpretation of $\tau^x_{j,\ell}$ is that a sourcing location ℓ needs ship $\tau^x_{j,\ell}$ units of a variety (x, ω) so that the location j receives one unit.

We normalize $\tau^x_{\ell,\ell} = 1$ for all locations ℓ and types x. Whenever $j \neq \ell$, we require that $\tau^x_{j,\ell} \geqslant 1$. We further require that the triangle inequality be satisfied: for any triplet of locations (j, k, ℓ), the following $\tau^x_{j,\ell} \leqslant \tau^x_{j,k}\tau^x_{k,\ell}$, so that there is no arbitrage opportunities in moving the goods around.

Variety Aggregation. Varieties are aggregated by type x with a CES function[5]. For each type of food, there is a unitary mass of varieties, which we denote by ω:

$$c^c_\ell = \left(\int_0^1 c^c_\ell(\omega)^{\frac{\nu^c - 1}{\nu^c}} d\omega \right)^{\frac{\nu^c}{\nu^c - 1}} \quad \text{and} \quad c^q_\ell = \left(\int_0^1 c^q_\ell(\omega)^{\frac{\nu^q - 1}{\nu^q}} d\omega \right)^{\frac{\nu^q}{\nu^q - 1}} \tag{1}$$

where $c^x_\ell(\omega)$ denotes the consumption of variety (x, ω) in location ℓ. The CES structure delivers the ideal price indexes for each type of food as follows:

$$P^c_\ell = \left(\int_0^1 p^c_\ell(\omega)^{1-\nu^c} d\omega \right)^{\frac{1}{1-\nu^c}} \quad \text{and} \quad P^q_\ell = \left(\int_0^1 p^q_\ell(\omega)^{1-\nu^q} d\omega \right)^{\frac{1}{1-\nu^q}} \tag{2}$$

Our trade structure can be solved independently from the preference block, provided that this CES structure is imposed. Hence, we proceed with a general formulation and later specialize on the outer utility function.

[5] One alternative interpretation is that in each location there is a mass of competitive grocery shops that aggregate all varieties (x, ω) of each type x into a composite that the households buy by means of a CES production function.

Production. There is a single production factor, labor. Production is linear in labor in all sectors. The productivity on the outside good sector at location $\ell \in \mathcal{L}$ is given by Z_ℓ^o, so its inverse denotes the input requirement to produce a unit of output:

$$Y_\ell^o = Z_\ell^o N_\ell^o \tag{3}$$

where N_ℓ^o is the amount of labor allocated to such production. Letting w_ℓ denote the wage rate prevailing at the location ℓ. The cost of producing one unity of the outside good is given

$$\frac{w_\ell}{Z_\ell^o} \tag{4}$$

For the food goods, we model their production following Eaton and Kortum (2002) model. We denote by $Z_\ell^x(\omega)$ the efficiency of location ℓ in producing the variety ω of food type $x \in \{c, q\}$. The production technology takes the form of

$$Y_\ell^x(\omega) = Z_\ell^x(\omega) N_\ell^x(\omega) \tag{5}$$

so that the cost per unit for producing good variety (x, ω) at location ℓ is given by

$$\frac{w_\ell}{Z_\ell^x(\omega)} \tag{6}$$

Good sourcing. Consider the problem of a family living in location $j \in \mathcal{L}$ deciding where to source from. The cost in location $j \neq \ell \in \mathcal{L}$ to acquire a variety (x, ω) from location ℓ takes into account the production cost in location ℓ and the transportation costs from ℓ to location j, that is:

$$p_{j,\ell}^x(\omega) \equiv \left(\frac{w_\ell}{Z_\ell^x(\omega)} \right) \tau_{j,\ell}^x \tag{7}$$

Under the working assumption of perfect competition, location j buys from location ℓ if ℓ is able to supply at the lowest delivery cost, taking into account both production and transportation costs. The price that location j pays for the variety (x, ω) is the lowest among all potential sourcing

locations:

$$p_j^x(\omega) \equiv \min\left\{p_{j,\ell}^x(\omega) : \ell \in \mathcal{L}\right\} \tag{8}$$

Food Production Technology. We assume that the productivity draws follows the structure of Eaton and Kortum (2002). We denote by $Z_\ell^x(\omega)$ the productivity of variety (x,ω) at location ℓ, which we refer to as "EK term" below.

For each type of good-variety pair (x,ω), a location receives a productivity draw from a location-specific Fréchet probability distribution with the cumulative distribution function:

$$F_\ell^x(\tilde{z}) = e^{-T_\ell^x \tilde{z}^{-\theta^x}}. \tag{9}$$

The draws are independent across varieties (x,ω) within and across locations. The parameter T_ℓ^x, or "State of Technology," defines the mean productivity and reflects the absolute advantage of location ℓ for type x Eaton and Kortum (2002). The parameter θ^x, uniform across locations, governs the dispersion of productivity draws, with higher values implying narrower comparative advantages. As in Simonovska and Waugh (2014), θ^x represents the trade elasticity.

Price Determination. Below, we state the main results of the model and refer to a complete derivation in appendix B. As in Eaton and Kortum (2002), location j faces a probability distribution of prices of a variety

$$G_{j,\ell}^x(p) = 1 - e^{-[T_\ell^x (w_\ell \tau_{j,\ell}^x)^{-\theta^x}]p^{\theta^x}} \tag{10}$$

Because the productivity draws are i.i.d, this probability is the same for every variety (x,ω). This term gives the probability of location j being supplied by location ℓ with the price up to p for type x. Since location j buys from the lowest cost supplier, we next show the probability location j buy type-variety pair (x,ω) of a price of at most p. This requires that there is at least one location that supplies at the price not higher than p, as follows

$$G_j^x(p) = 1 - \prod_{\ell \in \mathcal{L}} [1 - G_{j,\ell}^x(p)] \tag{11}$$

Plugging equation (10) into (11), we recover

$$G_j^x(p) = 1 - e^{-\Phi_j^x p^{\theta^x}} \tag{12}$$

where

$$\Phi_j^x \equiv \sum_{\ell \in \mathcal{L}} T_\ell^x (w_\ell \tau_{j,\ell}^x)^{-\theta^x} \tag{13}$$

The term Φ_j^x shows how the State of Technology, T_ℓ^x, the input cost of production w_ℓ, and the trading frictions $\tau_{j,\ell}^x$ between each location ℓ and j ultimately shape the price distribution faced at the location j.

Price of Basket. As we shall see next, the state of these three forces *across all locations* and their interaction describes the price level in each location $j \in \mathcal{L}$. Equation (12) allows us to recover the ideal price indexes for each good type, in equation (2) , as follows:

$$P_j^x = \left(\sum_{\ell \in \mathcal{L}} T_\ell^x (w_\ell \tau_{j,\ell}^x)^{-\theta^x} \right)^{-\frac{1}{\theta^x}} \gamma^x \quad \text{for} \tag{14}$$

where γ^x is a time-invariant constant[6].

Trade Shares. We need to find out how trade flows are pinned down with given prices. To achieve that goal, let us start by computing the probability location j buys a given variety to location supplied by location $l \in \mathcal{L}$. Because the productivity draws are iid, and since there is a continuum of goods for each type, this probability turns out to be the share of goods that $\ell \in \mathcal{L}$ supply to $j \in \mathcal{L}$.

We denote by $\pi_{j,\ell}^x$ the fraction of goods of type x that location $j \in \mathcal{L}$ buys from location $\ell \in \mathcal{L}$, which is given by

$$\pi_{j,\ell}^x = \frac{T_\ell^x \left(w_\ell \tau_{j,\ell}^x \right)^{-\theta^x}}{\Phi_j^x} \equiv \frac{T_\ell^x \left(w_\ell \tau_{j,\ell}^x \right)^{-\theta^x}}{\sum_{\ell \in \mathcal{L}} T_\ell^x (w_\ell \tau_{j,\ell}^x)^{-\theta^x}} \tag{15}$$

In order to find out the total cost of these expenditures, we need to calculate the price of the

[6]This constant is equal to $\Gamma\left(\frac{\theta^x+1-\nu^x}{\theta^x}\right)^{\frac{1}{1-\nu^x}}$. $\Gamma(u)$ is the Gamma function, given by $\int_0^\infty x^{u-1}e^{-x}dx$, for $u > 0$. As we show later, once we apply logs and take differences, this constant disappears entirely

goods that location j bought from location ℓ. Due to the Fréchet distribution for the productivity draws, the distribution of paid prices faced by location $j \in \mathcal{L}$ of varieties coming from $\ell \in \mathcal{L}$ *conditional on* ℓ being the cheapest supplier turns out to be equal to the distribution of prices coming from $\ell \in \mathcal{L}$ to $j \in \mathcal{L}$, that is

$$\Pr\left\{p_{j,\ell}^{x}(\omega) \leqslant \tilde{p} \mid p_{j,\ell}^{x}(\omega) \leqslant \min_{k \in \mathcal{L}_{-\ell}} p_{j,k}^{x}(\omega)\right\} = G_{j}^{x}(\tilde{p}) \tag{16}$$

The result in (16) implies that the share of expenditures on type x in the location j that is supplied by location ℓ is also given by $\pi_{j,\ell}^{x}$.

3 Equivalent Variation

In what follows, we borrow insights from the standard demand theory, in the spirit of Fajgelbaum and Khandelwal (2016) to shed light on why the separation between the trade and the demand blocks we propose is particularly useful. In particular, as we show next, because of free mobility of labor across sectors, and because the changes in productivity affect only the agricultural sector, by assumption, income in terms of the outside good is constant. Hence, changes in utility from the productivity in the food sector come from the changes the relative price of food alone.

3.1 Climate change through the lens of the Model

The average *potential* productivity of the food-producing sectors is defined to be $\mu_{\ell}^{x} \equiv \mathbb{E}[Z_{\ell}^{x}(\omega)]$. Because the draws for each $\omega \in [0,1]$ comes from a Frechét distribution, this average productivity relates to T_{ℓ}^{x} according to the formula

$$T_{\ell}^{x} = \left[\mu_{\ell}^{x}\right]^{\theta^{x}} \kappa^{x} \tag{17}$$

where κ^{x} is a time-invariant constant common to all locations[7]. In what follows, we will assume that climate change affects T_{ℓ}^{x}, by looking at μ_{ℓ}^{x}, which we can read from the GAEZ dataset.

Let $\mathcal{V}_{i,j} \equiv V(P_{j}^{c}, P_{j}^{q}, y_{i})$ be the indirect utility of an individual with income y_{i} in a location j,

[7]This constant is equal to $\Gamma\left(\frac{\theta^{x}-1}{\theta^{x}}\right)^{-\theta^{x}}$. $\Gamma(u)$ is the Gamma function, given by $\int_{0}^{\infty} x^{u-1}e^{-x}dx$, for $u > 0$.

where prices are P_j^c and P_j^q. Notice that because the outside good is the numeraire, its prices do not appear in the indirect utility. Taking the log of $\mathcal{V}_{i,j}$ and its total derivative with respect to log prices and log income, we have:

$$\widehat{\mathcal{V}}_{i,j} = \sum_{x \in \mathcal{X}} \frac{\partial \log(\mathcal{V}_{i,j})}{\partial \log P_j^x} \widehat{P}_j^x + \frac{\partial \log(\mathcal{V}_{i,j})}{\partial \log y_i} \widehat{y}_i \tag{18}$$

where we use the convention $\hat{z} \equiv d\log(z)$ representing the log change in a variable z. Let $\text{EV}_{i,j}$ be the equivalent variation associated with the prices changes as the proportional change in income, at pre-shock prices, which would generate the same change in utility as the total derivative above:

$$\widehat{\mathcal{V}}_{i,j} = \frac{\partial \log(\mathcal{V}_{i,j})}{\partial \log y_i} \text{EV}_{i,j} \tag{19}$$

Here, $\text{EV}_{i,j}$ is the variation in income that would be necessary to achieve the same variation in utility that would have happened from the variation in prices and income above, that is $\widehat{\mathcal{V}}_{i,j}$.

We recover the following formula for the Equivalent Variation using Roy's Identity, while noticing that $\hat{y}_i = 0$ since in our setting, due to the free mobility of labor across sectors and the assumption that Z_ℓ^o is not affected by Climate Change, income is constant[8]:

$$\text{EV}_{i,j} = \sum_{x \in \mathcal{X}} -\text{s}_{i,j}^x \widehat{P}_j^x \tag{20}$$

where $s_{i,j}^x$ is the expenditure share on good x with income i at location j, at the pre-shock prices. The interpretation of $\text{EV}_{i,j}$ is the consumer's willingness to pay to avoid the price changes.

The prices changes $\widehat{P}_j^x$ for each x happen due to changes in the productivity in each crop, in each location. Through the lens of our model, we map climate change into a change in the parameter μ_ℓ^x, implemented as a change the parameter T_ℓ^x, per equation (17). In particular, we have

$$\widehat{P}_j^x = \sum_{\ell \in \mathcal{L}} \frac{\partial \log(P_j^x)}{\partial \log(\mu_\ell^x)} \widehat{\mu}_\ell^x \tag{21}$$

[8] It is straightforward to relax this assumption.

Using (14), (17), and (15) we have

$$\frac{\partial \log(P_j^x)}{\partial \log(\mu_\ell^x)} = -\pi_{j,\ell}^x \tag{22}$$

So that the change in the price of basket of type x in location j relates to changes in the average productivity in location ℓ according to the trade share, $\pi_{j,\ell}^x$. Using this result in (20), we recover

$$\text{EV}_{i,j} = \sum_{x \in \mathcal{X}} \text{s}_{i,j}^x \sum_{\ell \in \mathcal{L}} \pi_{j,\ell}^x \widehat{\mu}_\ell^x \tag{23}$$

Equation (23) shows that the equivalent variation depends on the components. First, it depends on the expenditure share on type x under income i and location j , $s_{i,j}^x$. This information is recoverable from the data, by means of exploit the latest consumer expenditure survey, provided a classification for what should be in each basket x. The second component is the trade-share between location j and all other suppliers locations ℓ, given the the type x, which is $\pi_{j,\ell}^x$. This component is not observed directly in the intra-national data, and one needs to estimate it. Finally, the last component is the proportional change in the average *potential* productivity, $\widehat{\mu}_\ell^x$.

Next, we show how we perturb the model in order to recover the estimate for $\pi_{j,\ell}^x$. The key idea is to introduce a transitory weather shock that is observed in the data and can be useful to backout these estimates, provided the structure of the model and the available data.

4 Recovering the Trade Frictions

Our main goal in this section is to estimate the trade shares, which are not directly observed in the data. In order to do so, we introduce a transitory component to agriculture productivity that depends on the realization of a weather shock.

Weather Shocks. At each period, a weather shock realizes, which we denote by $\boldsymbol{h} \equiv \{h_\ell\}_{\ell \in \mathcal{L}}$, where a location ℓ receives h_ℓ. As we explain below, these weather shocks affect the productivity of food-producing sectors, affecting their production costs. For simplicity, we assume that these heat shocks do not affect the productivity of the outside sector. In what follows, we suppress h_ℓ from the notation to limit notation clutter.

In this perturbed environment, there are two terms that define the productivity of the food-producing sectors. The first is a permanent productivity that follows the structure of Eaton and Kortum (2002), while the second term captures the transitory effects of heat in the productivity of crops.

We denote by $\tilde{Z}_\ell^x(\omega)$ the permanent productivity of variety (x,ω) at location ℓ, which we refer to as "EK term" above. The second term accounts for how the weather realizations affect productivity temporarily, and we denote it by $G^x(h_\ell)$. We emphasize that the first term is time-invariant and the second is stochastic. The "effective efficiency" $Z_\ell^x(\omega)$ is then

$$Z_\ell^x(\omega) = \underbrace{\tilde{Z}_\ell^x(\omega)}_{\text{EK term}} \times \underbrace{G^x(h_\ell)}_{\text{Weather Shock}} \tag{24}$$

Different realizations of the weather variable h_ℓ map into different levels of "effective productivity". These effects are invariant to the location — there is no subscript ℓ in the function $G^x(\cdot)$— but we allow food types to have different sensitivities to heat. The unitary cost of production variety (x,ω) is given by

$$\tilde{w}_\ell^x \equiv \frac{w_\ell}{G^x(h_\ell)} \tag{25}$$

From the expressions above for the prices and trade shares, Equations (14) and (15), the key change is the replacement of w_ℓ by $\tilde{w}_\ell^x$:

$$P_j^x = \left(\sum_{\ell\in\mathcal{L}} T_\ell^x (\tilde{w}_\ell^x \tau_{j,\ell}^x)^{-\theta^x}\right)^{-\frac{1}{\theta^x}} \gamma^x \quad \text{and} \quad \pi_{j,\ell}^x = \frac{T_\ell^x \left(\tilde{w}_\ell^x \tau_{j,\ell}^x\right)^{-\theta^x}}{\sum_{\ell\in\mathcal{L}} T_\ell^x (\tilde{w}_\ell^x \tau_{j,\ell}^x)^{-\theta^x}} \tag{26}$$

The log linearity of the price of the basket and the trade shares allows us to derive link between the incidence of heat and changes in prices. We exploit this link to recover estimates of these trade frictions.

4.1 From Heat Shocks to Prices Changes

In this section, we show how we recover estimates of trade costs for each type of food good. First, we develop the results that we need in order to run the structural regression.

For a type x of food, the model implies a close relationship between logarithmic changes in price and the occurrence of heat in *every* location. In the model, heat reduces the productivity of each sector, effectively increasing the unitary cost of production: more labor is required to produce one unit of output. Then, because the locations trade among themselves, the higher production cost in *one* location translates into higher bundle cost in *all* other locations, with the relative importance given by the trade shares. Next, we formalize this intuition.

Consider a location j of interest and a location ℓ that receives a heat shock. The price at the location j increases with an increase in the cost of production at the location ℓ according to

$$\frac{\partial \log(P_j^x)}{\partial \log(\tilde{w}_\ell^x)} = \pi_{j,\ell}^x \tag{27}$$

Equation (27) shows that the elasticity of the price index at j with respect to production costs at location ℓ is given by the expenditure share of location j from location ℓ. Intuitively, location j is more exposed to shocks at ℓ with the higher importance of ℓ as a supplier. This production cost increases with the realization of heat. By our formulation, this implies

$$\frac{\partial \log(\tilde{w}_\ell^x)}{\partial h_\ell} = -\frac{\partial \log(G^x(h_\ell))}{\partial h_\ell} \equiv \eta^x \tag{28}$$

This delivers a single semi-elasticity that is one output of our estimation procedure. Notice that we assume, for simplicity, that η^x is homogeneous between locations. This is an identification assumption. Putting all together, we recover

$$\begin{aligned}\frac{\partial \log(P_j^x)}{\partial h_\ell} &\equiv \frac{\partial \log(P_j^x)}{\partial \log(\tilde{w}_\ell^x)} \frac{\partial \log(\tilde{w}_\ell^x)}{\partial h_\ell} \\ &= \pi_{j,\ell}^x \times \eta^x\end{aligned} \tag{29}$$

The logarithm increase in the cost of a basket x in a location j goes up with a shock realized at location ℓ with two components. The first is how much location j is exposed to shocks in ℓ through

trade, $\pi^x_{j,\ell}$ multiplied by how much the production cost in ℓ increases upon the realization of heat, at the margin.

This gives the price change up to a first-order approximation, with "one unit" of the h_ℓ. In reality, shocks would affect each region. To take all this into account, we take the total derivative of the price with respect to heat shocks in each location and sum it across all locations.

$$\Delta \log(P^x_j) \approx \eta^x \sum_{\ell=1}^{L} \pi^x_{j,\ell} \Delta h_\ell \tag{30}$$

In our approach is then to use variation from observed price changes and heat shock realizations to infer the trade shares $\pi^x_{j,\ell}$. The key idea is to use the structure of these trade shares in the model, together with observables in the data to recover the trade costs, allowing us to retrieve the missing shares. Toward this goal, we next describe the data we use.

4.2 Weather Data

Our weather satellite data is extracted from Copernicus Climate Change Service (2019) for the 1950-2021 period. We use the hourly average land temperature at the raster level of 0.1° by 0.1°[9]. We calculate the number of days of exposure to temperatures above 30°C/86°F at the quarterly level. We convert the raster-level exposure data to the municipal level by computing the municipal average exposure over the rasters contained in the municipal boundary. Ultimately, we calculate the weighted state-level average of exposure, weighting municipalities by the average annual value of municipal crop production from 1999 to 2021. The crop production data comes from the Systematic Survey of Agricultural Production collected by IBGE, which we describe in more detail in the Appendix A.2.

We choose 30°C as our temperature threshold, given the adverse effects that temperatures above this threshold have on crop yields, as well documented in Schlenker and Roberts (2009). They find non-linear effects of exposure to high temperatures on maize, cotton, and soybean yields. We validate this choice for the temperature threshold. As documenting the link between heat exposure and crop yields is not entirely novel in the literature, we include them in the Appendix A.2. Our analysis shows a contraction in crop yields after exposure to temperatures above $30^\circ C$

[9]Equivalent to 11 by 11kms, or 6.5 by 6.5 miles. Owing to the curvature of the earth, the area covered in the grids increases as we approach the equator line.

in the crop growing season. The estimates are statistically significant and economically relevant. After controlling for state-year factors, the semi-elasticity is around -0.4% for rice, -0.6% for soybeans, and 0.6% for beans.

4.3 Consumer Price Index Data

We use data from the official Consumer Price Index (CPI) in Brazil, taken from IBGE[10]. The most detailed data are available at the "sub-item" level (e.g., banana, bus fare, t-shirt) at the monthly frequency, which aggregates into baskets called "items" (e.g., fruits, public transportation, youths apparel), and further aggregates named "groups"(e.g., food and beverages, transportation, apparel). Nationwide, IBGE tracks a basket of sub-item prices, mimicking the average consumption basket of a family with income ranging from 1 to 40 minimum wages and living in urban areas[11].

The raw microdata consists of a panel of locations and price changes at sub-item, item, and group levels, together with the monthly weights. Our sample starts in August 1999, a date that we chose given the history of hyperinflation before 1994 and the pegged exchange rate from mid-1994 until early 1999. The last observation date is December 2023. The panel is unbalanced, with 11 locations at the beginning of the sample and 16 at the end of the sample. A location is either a metro area or a municipality (state capital), and there is at most one location per state. More details in these locations, and their relevance are relegated to Appendix A.3.

The price levels are not directly available, so we construct price indices. For each location, we use the raw microdata to construct the price level for a variety of baskets. For a given basket, we renormalize the weights of the sub-items that are part of the basket so that they sum up to one hundred and compute the weighted average inflation. Then, we recover the price index for each basket by compounding its inflation over time. We refer to appendix A.3 for further details on the CPI data and the steps taken to recover the price levels.

We borrow a tradability classification from the Brazilian Central Bank (BCB) in order to construct low-trade-cost and high-trade-cost food baskets. The BCB calls goods "tradable" and "non-tradable", respectively. In the classification, "non-tradable" is not *literal*: these are goods and

[10] In Portuguese, it is the IPCA — Índice de Preços ao Consumidor Amplo.

[11] This income range covers around 90% of the families in the latest Consumer Expenditure Survey, from 2017-2018. The national minimum wage in 2018 was R$ 954. The average commercial exchange rate against the U.S. dollar fr 2018 was approximately R$ 3,65 per US$, so the minimum wage was approximately US$ 260 in 2018.

services that are produced and consumed primarily domestically, with a minor role played by international trade. Examples of "Tradable Food" are soybean, rice, wheat, sugar, and their derivatives, while beans and fresh food such as tomatoes, lettuce, and kale are examples of "Non-tradable Food". We refer to appendix A.4 for further details on the BCB classification. In order to avoid any confusion, we call the "tradable" basket as low-trade-cost "LTC" and the "non-tradable" as HTC.

4.4 Structure for the Trade Shares

We use the functional form for the trade shares shares from Equation (15) in a non-linear estimation approach. Specifically, we estimate the parameters $[T_\ell^x]$, wages $[\tilde{w}_\ell^x]$, and a parameter θ^x, while imposing a functional form on trade frictions $[\tau_{j,\ell}^x]$ based on observables. We then maximize the fit of the model by aligning it with this structure.

For the trade cost functional form $\tau_{j,\ell}^x$, we adopt a straightforward approach, using driving time between state capitals with a constant elasticity. A non-linear least squares method allows us to estimate the elasticity δ^x separately for each food type.

The following sections outline the data sources and processing methods used to construct the trade shares

4.4.1 Technology Level T_ℓ^x

The State of Technology parameter T_ℓ^x relates to the average *potential* productivity of a location ℓ for type x, as Equation (17) highlights. It is important to note that this Equation does not allow us to identify the parameter θ^x separately. This is a common feature in the trade models, where some parameters cannot be separately identified. Hence, we take a value from the literature, in particular Astorga-Rojas (2024) and Albert et al. (2024).

The GAEZ data come in raster form for 53 crops, for the historical crop yields for the period of 1981-2010. The unit of measurement is kilograms per hectare. For each of the these 53 crops, we calculate the potential yield at the state level. There are two adjustments that we need to perform with these data so that we can arrive at an estimate for T_ℓ^x.

First, since our model considers labor as the sole production factor, we must translate land

productivity into labor productivity. To accomplish this, we rely on data from Brazil's most recent agricultural census, which took place in 2017. We utilize the national average for input requirements per crop, which indicates the number of workers employed per unit of land. Two fundamental assumptions underpin this approach. Firstly, a Leontief production function is employed, implying a fixed ratio between land and workers across different locations. This ratio varies based on the crop: some crops require more land, while others demand more labor. Secondly, it is assumed that land is relatively abundant, implying that production is contingent on labor allocation rather than the land's quantity.

The subsequent adjustment involves incorporating averaging. This step is crucial as the units after the initial adjustment, and even before, do not align across different crops, resulting in kilograms per worker. By converting land productivity into worker productivity measured in kilograms, we address the issue by multiplying labor productivity by the historical average price per crop at the national level. Consequently, we map μ_ℓ^x to the revenue productivity within the dataset. The source of the crop price data is the *Systematic Survey of Agricultural Production* (SSAP)[12]. We used the ratio between the total production value divided by the total production quantity at the national level per year from 2002 to 2022[13]. Then, we take the average over the years. The use of national price is intended to mitigate the issue of the state price incorporating the trade frictions themselves, as the local price in isolated places tends to be higher.

For the second adjustment, we aligned the FAO *potential* crop yields with those monitored by the SSAP. Altogether, there are 29 crops that were mapped between these datasets. These 29 crops are categorized as either low-trade-cost or high-trade-cost based on their names' correspondence with CPI food items. Specifically, 17 crops fall under LTC, while 12 are designated as HTC. These matched crops represent on average, across time, 90 percent of all crop production value and 95 percent of land utilization nationwide. Appendix A.5 contains a complete list of these crops, along with further details on these adjustment factors.

Finally, since the trade share in Equation (15) is homogeneous of degree 0 in the vector of productivities, we choose the state of São Paulo as a reference and normalize the other states T_ℓ^x as a ratio of the level of São Paulo. The resulting measure for μ_ℓ^x for each food type is show in

[12] In Portuguese, "Levantamento Sistemático da Produção Agrícola".

[13] The records for 2001 and before of the prices were measured as local currency per unit or bunch for some crops, especially fruits.

Appendix A.5.

4.4.2 Wage level $\tilde{w}_\ell^x$

We borrow wages from the Continuous National Household Sample Survey[14] conducted by the IBGE. This is a household survey that started in 2012 and is ongoing. The data is released at the state level at a quarterly frequency.

We make two decisions. First, similarly to the parameters T_ℓ^x, the trade share is Equation (15), it is homogeneous to zero degree in the wages vector. Hence, we work again with São Paulo as a reference state: the wage cost normalized to 1 and fed into the estimation procedure the relative wage of all states to the level in São Paulo.

Furthermore, given that the temporal coverage is less than half of that provided by the CPI data, utilizing the time series of relative wages would result in a loss of approximately half of our sample size. To address this limitation, we opt to use a singular representative value for the wage in each state. Specifically, we compute the varying ratios of relative wages compared to São Paulo and subsequently determine the average of this time series.

Through the lens of our model, one might interpret this strategy as follows: we take a first-order approximation of this trade shares with respect to $\tilde{w}_\ell^x$ around a zero heat shock position $\boldsymbol{h} = \mathbf{0}$ and let fixed effects and the residuals soak the approximation error. If this relative rate shows any particular seasonal pattern, the state-season fixed effects that we include in the regression would capture such a pattern. The series we use is the average usually received wage in all occupations. For our purposes, this serves as a proxy for Z_ℓ^o.

There are two main implications resulting from taking this approach. First, since the wage is constant, it follows that the trade shares are constant - the state of technology, trade frictions, and the parameter θ^x are assumed to be invariant in this stage. In reality, these trade shares probably fluctuate, but these are all unobserved fluctuations. Second, the wage level that we input into the estimation procedure is the same regardless of the type of food. The values for the wage we use for each state can be found here in Appendix A.5.

[14] PNAD Contínua, in Portuguese

4.4.3 Trade Elasticity θ^x

There is great variability in the estimates of trade elasticity in the empirical applications of trade models. As discussed above, we borrow the trade elasticity parameter θ^x from Astorga-Rojas (2024). The author leverages the construction of Brasilia and the project to connect the newly created national capital city to other state capitals as a natural experiment. Using archival data with state-to-state trade flows from 1942 to 1949 and 1968 to 1974; the author recovers an estimate for the trade elasticity from a gravity equation using the construction plan for roads connecting Brasilia to other state capitals as an instrument. The value he finds is $\theta^x = 3.39$. The value is the same used in Albert et al. (2024) and within the range proposed in the literature. Notice that we use the same trade elasticity for both types of food.

Pellegrina (2022) relies on archival data from Brazil together with the price of agricultural goods finds a trade elasticity θ^x around 3.90 for perishable agricultural products (vegetables and fruits), and θ^x around 5.1 and 5.6 for cereals (rice, soybeans, corn, and wheat) and other non-perishable agricultural products, respectively. The value we use, $\theta^x = 3.39$, is within the range proposed in Simonovska and Waugh (2014) and similar to the value of 4 commonly assumed when this parameter is not directly estimated. Ramondo et al. (2016) uses a value of 4 when studying domestic frictions in the US.

4.4.4 Trade Frictions Specification

We need to discipline one matrix of trade costs per type of food, totaling values of parameters $27 \times 27 \times 2$. Given the assumed full integration within each state ($\tau^x_{j,j} = 1$), we impose symmetry ($\tau^x_{j,\ell} = \tau^x_{\ell,j}$) of the trade costs reduces the number of parameters. The lack of trade data within subparts of a nation is common (Ramondo et al., 2016; Pellegrina, 2022; Sotelo, 2020). Approximately two thirds of the cargo in Brazil is conducted by trucks via roads (World Bank, 2022),we impose that these trade costs are a function of the driving time between state capitals.

Precisely, the functional form that we use is

$$\log(\tau^x_{j,\ell}) = \begin{cases} 0 & \text{if } j = \ell \\ \delta^x \log(d_{j,\ell}) & \text{if } j \neq \ell \end{cases} \tag{31}$$

The variable variable $d_{j,\ell} \geqslant 0$ is a measure of distance between the capital of states j and ℓ. As we explained in the model, we set $\tau_{j,\ell} = 1$ whenever $j = \ell$. For all the other cases, the distance is non-zero, and we assume that the trade friction $\tau^x_{j,\ell}$ exhibits a constant elasticity with respect to the measure of the distance. We allow this elasticity to be different for the two types of food goods, low-trade-cost and high-trade-cost.

We measure the distance $d_{j,\ell}$ by the driving time, in hours, from the capitals of j and ℓ. We collect this information from Open Street Maps in July 2024. Similarly, Pellegrina (2022) uses Google Maps data for the driving time for some of his estimation. The information contains the driving distance in kilometers and the driving time in hours - which allows us to compute the average speed, measured in kilometers per hour. Since there is substantial heterogeneity in the average speed between locations, we interpret this as a sign of heterogeneous road quality across the nation.

Table 1: Descriptive statistics for alternative measures of Driving Distance

Measure	Origin Capital	N	Mean	SD	Min	p25	p50	p75	Max
Driving Distance, km	All	702	2619	1443	112	1534	2430	3597	6702
	Manaus	26	4050	1403	754	3420	4392	4988	6020
	São Paulo	26	2152	1220	408	956	2309	2935	4653
	Porto Alegre	26	2975	1312	473	1884	3427	4000	5236
Driving Time, hours	All	702	38	22	2	21	34	53	100
	Manaus	26	65	20	13	56	68	77	90
	São Paulo	26	30	19	6	13	30	39	73
	Porto Alegre	26	41	19	6	26	45	53	81
Average Speed, km/hour	All	702	70	6	52	66	71	75	82
	Manaus	26	62	4	52	60	62	65	67
	São Paulo	26	73	5	63	69	74	77	81
	Porto Alegre	26	74	4	65	70	75	77	78

Notes: The table displays the statistics for driving distance, driving time and average speed between all pairs of state capitals in Brazil. There are 27 states, with 702 (27×26) unique pairs of origin-destinations. Swapping the order of origin and destination within the pair might lead to different estimates for the three variables shown in the table. The reason is that the exact route might not be two-ways all along. The differences are usually smaller than 1%, considering absolute deviation from the mid-point. Manaus is the capital of Amazonas, in the Norte Region in the Amazon. São Paulo is the capital of São Paulo and Porto Alegre is the capital of Rio Grande do Sul, the state most to the South. Data is from Open Street Maps, collected in July 2024. p25 stands for the percentile 25% in the distribution, while p75 stands for the percentile 75%.

Table 1 shows some descriptive statistics for all unique origin-destination pairs of state capitals ("All"), and some selected capitals. Brazil is a large country, so driving distance measured in

kilometers between state capitals go as high as 6700 km. The median travel time is 34 hours, spamming from 2 to 100 hours. There is substantial dispersion in road quality, proxied by the average speed: the interquantile interval for the average speed is 9 km, from 75km/h to 66km/h, while the range of this variable is from 52km/h to 82km/h.

In order to further illustrate the dispersion is road quality and remoteness, we include in Table 1 three state capitals for reference. We choose Manuas, the state capital of Amazonas, to be a representative location of a reasonably dense location that is somewhat far from other state capitals. Manaus is situated in the center of the Amazon rainforest, an area that remains fairly secluded, with road travel speeds being quite modest. The median driving time from Manaus to other capitals is 68 hours, with the median speed being 62 km. It is not only about how distant Manaus is, but how *difficult* or costly, in time, to get there.

We added two other capitals for easing the comparison. São Paulo, the capital of the homonymous state, is the richest capital and amounts to the most populated capital. The median and average driving time is 30 hours, with a median speed of 74 km/hour. Porto Alegre is the state capital of Rio Grande do Sul, the state that is most to the south. Almost by construction, Porto Alegre is "far" from many states, specially the ones from the North and Northeast. This pattern can be seen from the driving distances and driving times, that are offset relatively to São Paulo, that is somewhat more central. It is somewhat remarkable that the average speed departing from São Paulo or from Porto Alegre are very much lined up.

Having gotten a sense of these differences in the driving time, we next describe the estimating regression that we run to recover the trade costs.

4.4.5 Estimating Equation and Results

We are now in place to implement our specification, as in (30). The estimating regression is

$$\ln(p^x_{j,t}) - \ln(p^x_{j,t-1}) = \eta^x \sum_{\ell=1}^{L} \pi^x_{j,\ell} \text{Heat}_{\ell,t} + \xi_t + \chi_{\ell,s} + \epsilon_{j,t} \tag{32}$$

The dependent variable is the log change in prices for a basket x in a location j between period t and $t-1$. The baskets that we consider are the low-trade-cost and the high-trade-cost food, from the CPI data. The independent variable is a weighted average of the heat across all states, with the

weights given by the trade shares between the reference state j and all others, indexed by ℓ. The $\text{heat}_{\ell,t}$ variable is the number of hours, measured in days, state ℓ was exposed to the temperature of $30^{\circ}C$ during quarter t. We run the regression at the quarterly frequency.

Because there is variation in the price data that are non-necessarily related to the realizations of heat, we further include two types of fixed effects. First, ξ_t is the quarterly date fixed effect. This term captures forces that push inflation up and down in all locations regardless of the heat shocks, such as the business cycle or the nominal interest rate. In addition, we also have a fixed effect interacting with location and season, namely $\xi_{\ell,s}$. In Brazil, the seasons are summer, fall, winter, and spring from quarter one to four of the calendar year. These dummies are meant to capture seasonal patterns that are specific to each location. Because Brazil is very vast across the latitudes and relatively to the east coast, there is substantial heterogeneity in the seasonal patterns of heat — and hence prices. For example, locations in the North and Northeast are closer to the Equator line and then to be relatively warmer.

The multiplying coefficient η^x is an outcome of the procedure. This is the semi-elasticity of the yields in a given location with respect to the heat that is realized at that location, as in Equation (29). We first discuss the results regarding δ^x, later focusing on the discussion for η^x.

Table 2 shows the results from the non-linear least square estimate of Equation (32). For goods classified as low-trade-cost, the elasticity of the trade friction with respect to the driving time is about 0.30, while this elasticity is around 0.56 for the high-trade-cost food goods. We bootstrapped the confidence interval for this elasticity using 300 repetitions, with 95% of the sample clustered at the state level. The coefficients are statistically different from zero and each other.

Table 2: Regression (32), estimated by Nonlinear Least Squares

	LTC Food Goods	HTC Food Goods
$\log(d_{j,\ell})$, δ^x	0.303***	0.561***
	(0.053)	(0.083)
Observations	1,211	1,211
R-squared	0.89	0.82
States	16	16
Fixed Effects:		
Quarterly Date	✓	✓
State-Season	✓	✓

Note: Bootstrapped standard errors clustered at State level. We performed 300 repetitions, with 95% of the sample for each state. Significance levels: $p <$ *** 1%

By construction, these elasticities get the dynamics of both price and heat shocks from the data as close as possible to the ones that the model implies. We now offer some heuristic explanations on why the ordering of these elasticity turns out to be consistent with the ordering low-versus-high trade cost in the classification.

Figure 1: Spatial Correlations of Heat and Inflation

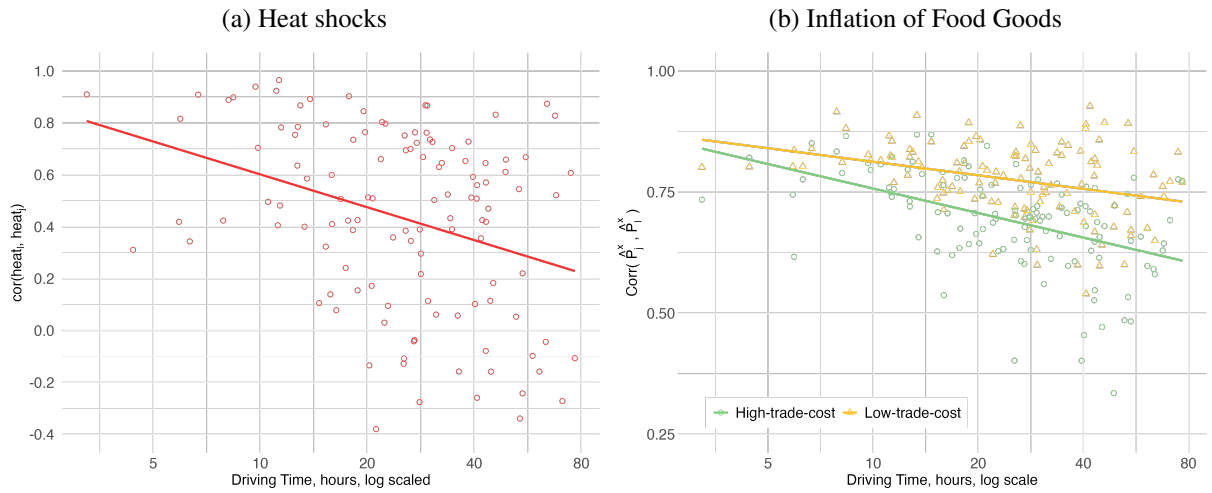

Note: For both panels, the horizontal axis is the driving time between the pair of state capitals, in log scale. Panel (a) shows the spatial correlation of the heat shocks. The vertical axis is the correlation across the time series of these heat shocks for each pair of states. Panel (b) shows the correlation of food good inflation for each pair of states, by tradability classification. Here $\hat{P}_j^x \equiv \log(P_t^x) - \log(P_{t-1}^x)$. In yellow, we have the low-trade-cost food goods, while in green we have the high-trade-cost goods.

Heat shocks are naturally spatially correlated. Panel (a) of Figure 1 shows the correlation of heat shocks between pairs of states plotted against the driving time between their capitals. Nearby states, with shorter driving times, experience similar shocks, leading to high correlations.

Panel (b) of Figure 1 reveals a less intuitive pattern: nearby locations also exhibit closely related inflation dynamics, with correlations decreasing as driving time increases. Unlike heat shocks, inflation correlations remain above 0.50 even for distant locations. This persistence reflects other nationwide drivers of inflation, such as monetary policy and the business cycle[15].

A notable feature in Panel (b) is that the decline in inflation correlation is sharper for high-trade-cost (HTC) food goods.[16] Due to higher trade costs, states are more likely to source HTC goods from nearby states, making local inflation more sensitive to local conditions. Since heat shock correlations drop off quickly with distance, inflation correlations for HTC goods decline faster than for low-trade-cost goods. Thus, the higher elasticity δ^x for HTC goods aligns with the observed correlation patterns of both heat shocks and inflation across the cross-section.

Table 3: Outcome for regression (32) under alternative regressors

Dependent variable: $100 \times (\log(p^x_{j,t}) - \log(p^x_{j,t-1}))$				
	LTC Food (1)	HTC Food (2)	LTC Food (3)	HTC Food (4)
$\text{Heat}_{t,j}$	0.049***	0.104*		
	(0.017)	(0.058)		
$\sum_{\ell=1}^{L} \pi^x_{j,\ell}\text{Heat}_{t,\ell}$, η^x			0.113***	0.120*
			(0.039)	(0.066)
Observations	1,211	1,211	1,211	1,211
R-squared	0.89	0.82	0.89	0.82
States	16	16	16	16
Fixed Effects:				
Quarterly Date	✓	✓	✓	✓
State-Season	✓	✓	✓	✓

Note: Robust Driscroll-Kraay standard errors. Significance levels: $p <$ *** 1%, ** 5%, * 10%. Columns (1) and (2) show the result of the regression in (32) by imposing $\pi^x_{j,j} = 1$, that is including only the own shock to state j. Columns (3) and (4) exhibit the results for the weighted average of the heat shocks and with the estimation conducted by NLS.

A notable feature in Table 3 is the change in estimated coefficients when comparing regressions using only own-state shocks versus those including shocks from all states. Since states trade with one another, heat shocks affecting sourcing states influence the price dynamics of destination states. By considering only the own-state shock, relevant variables are omitted, leading to biased

[15] Although not depicted in the figure, components that are entirely immobile, such as "food away from home," exhibit an average correlation of 0.30, which remains constant regardless of driving time.

[16] This pattern is supported by regression analysis showing statistically different slopes for high- and low-trade-cost goods.

coefficients in columns (1) and (2). Accounting for shocks from all states, through the structure of the model for $\pi^x_{j,\ell}$, effectively incorporates these variables under the assumption that η^x remains consistent across states.

The relationship between the coefficients under different specifications also connects to the elasticity estimate δ^x for each food type. For high-trade-cost (HTC) goods, the elasticity δ^q is relatively high, resulting in low trade shares for states other than the own state ($\ell \neq j$). Consequently, the coefficients in columns (2) and (4) are similar, reflecting a near-autarky situation for HTC goods. In contrast, for low-trade-cost (LTC) goods, the lower elasticity δ^c leads to more interstate trade, with $\pi^c_{j,j}$ deviating from unity. As a result, including previously omitted variables causes a significant shift in the estimated coefficients between columns (1) and (3). Interestingly, the resulting semi-elasticity of crop yields to heat, η^x, remains consistent across both food types.

The heat elasticity η^x, detailed in Table 3, reflects short-term elasticity, measuring the change in log yields from one additional day above $30^{\circ}C$ in a quarter. It is not intended to predict long-term productivity changes under climate change scenarios.

While η^x is not useful for counterfactual exercises, it validates the model by aligning implied semi-elasticities of crop yields to heat shocks with estimates from crop production data (Appendix A.2). Column (5) of Tables A.1, A.2, and A.3 report elasticities of 0.4%–0.6% for rice, soybeans, and beans, slightly higher than the 0.11% and 0.12% in Table 3, columns (3) and (4). Differences arise, for example, because crop production data are annual, focusing on critical growth cycles, while regression (32) is quarterly and averages sensitivity across crops and seasons.

Having recovered the estimates for the trade frictions, we are now ready to recover the trade shares, $\pi^x_{j,\ell}$, using equation (15). In the equivalent variation formula, equation (23), there are two other parts that can be obtained from the data. First, the food expenditure shares on type x at location j under income group i, $s^x_{i,jl}$ are recoverable from the latest consumer expenditure survey. Second, the changes in productivity, captured by $\hat{\mu}^x_\ell$, are drawn from the different scenarios for Climate Change.

While the first-order approach is transparent and intuitive, as the productivity changes become large, the approximation error may grow. And, as we show later in the text, these productivity shifts implied by climate change are significant. To deal with this, we specialize in a particular utility function that allows us to perform counterfactuals globally.

5 Preferences and Model Fit

5.1 Utility Function

We employ a non-homothetic utility function, which aligns the income's share allocated to food with observed data by depending on income. We use a Stone-Geary utility function that involves a minimum level of food consumption $\underline{c}^f$. Although the utility function remains consistent across regions, disparities in the costs of these minimum levels create state-specific effects. These are due to regional differences in food prices, leading to uneven minimum consumption costs. In addition, regional income variations influence the relative burden of these costs on households in different states.

$$\mathcal{U}(c^o_{i,\ell}, c^f_{i,\ell}) = (1-\alpha^f)\log(c^o_{i,\ell}) + \alpha^f \log(c^f_{i,\ell} - \underline{c}^f) \tag{33}$$

where $c^o_{i,\ell}$ is the consumption of the outside good, $c^f_{i,\ell}$ is the food consumption and $\underline{c}^f$ is the minimum consumption of good. The indices (i,ℓ) refer to income i in location ℓ.

Food is a composite of low- and high-trade-cost food CES aggregators. We assume for now that this composite is a Cobb-Douglas function, as follows:

$$c^f_{i,\ell} = \alpha^c \log(c^c_{i,\ell}) + \alpha^q \log(c^q_{i,\ell}) \tag{34}$$

$c^c_{i,\ell}$ is the consumption of the low-trade-cost food composite and $c^q_{i,\ell}$ is the high-trade-cost food composite, with income i in location ℓ. This formulation allows us to write the price of food in location ℓ as a function of the price of each type-specific basket:

$$P^f_\ell = \left(\frac{P^c_\ell}{\alpha^c}\right)^{\alpha^c} \left(\frac{P^q_\ell}{\alpha^q}\right)^{\alpha^q} \tag{35}$$

Notice that the income level does not appear in this price: regardless of income, the price of food depends on the location ℓ where it is consumed. However, due to the non-homotheticity of the utility function, households with different incomes in the same location will face distinct burdens

to pay for the floor consumption of food. Precisely, the food expenditure share is given by

$$s^f_{i,\ell} = \alpha^f + (1-\alpha^f)\underbrace{\frac{P^f_\ell \underline{c}^f}{y_{i,\ell}}}_{\psi_{i,\ell}} \tag{36}$$

The term $\psi_{i,\ell}$ captures the subsistence share: the share of income required to pay the floor consumption of food. Given the Cobb-Douglas aggregator for the food composite, the food expenditure share for each type is given by

$$s^x_{i,\ell} = \alpha^x s^f_{i,\ell}, \qquad x \in \{c, q\} \tag{37}$$

Income. For the household in group i living in location ℓ, its income is simply their effective hours supply, $e_{i,\ell}$, times the wage prevailing at that location, w_ℓ. Because of free mobility across sectors, the wage is pinned down by the productivity in the outside sector, $w_\ell = Z^o_\ell$. The income $y_{i,\ell} = e_{i,\ell} w_\ell = e_{i,\ell} Z^o_\ell$.

5.2 Calibrating the Parameters

In our setting, since markets are competitive, prices are given by the marginal cost of production. Per equation (14), the prices of the baskets x are pinned down by State of Technology, T^x_ℓ, the wages $\tilde{w}^x_\ell$ and the trade frictions between locations, $\tau^x_{j,\ell}$. Because labor is fully mobile across the sectors, as in Costinot et al. (2016), the productivity of the outside sector Z^o_ℓ determines the labor cost in each state. As in Eaton and Kortum (2002), the income is hence exogenously given by the effective labor hours and the productivity Z^o_ℓ. The key implication is a separation between price determination and the demand side.

In contrast, the preference parameters and the income pin down the expenditure shares, for each household in each location. Given that the wage rate is governed by the productivity of the outside sector, Z^o_ℓ, introducing income heterogeneity is straightforward. We take the route of allowing households in each location to have heterogeneous endowments of effective labor hours. Facing the same hourly wage, the differences in effective labor hours generate mechanically income heterogeneity. Given the income for each household in each location, our goal is to calibrate

the preference parameters to match the food expenditure shares as closely as possible, taking as given the production structure and the implied prices. In our setting, we need to assign values for 6 parameters, two that are general $(\alpha^f, \underline{c}^f)$, and one pair for each type of food (α^x, ν^x) for $x \in \{c, q\}$. Next, we discuss the role of each of these parameters.

First, α^f approximates the food expenditure share as the subsistence ratio $\psi_{i,\ell}$ gets close to 0. Hence, this parameter is disciplined mostly by the behavior of the food expenditure share for the highest income decile. Conversely, when $\psi_{i,\ell}$ increases, so does the food expenditure share. Hence, the food expenditure share of the lowest-income decile disciplines the choice of $\underline{c}^f$, which drives $\psi_{i,\ell}$.

For the parameters of each food type, we set $\alpha^c = \alpha^q = 0.5$, based on average food expenditure shares. The CPI data includes both goods and services, such as "Food away from home," which falls under food services. In the BCB basket, the "tradable" (low-trade-cost) basket consists only of goods, while the "non-tradable" (high-trade-cost) basket includes both goods and services. Historically, the tradable basket accounts for around 50% of the food category in the CPI. Within the non-tradable basket, the representative family tracked by the official CPI (IPCA) allocates approximately 40% to goods and 60% to services. Since our model does not explicitly include food services, we incorporate the entire non-tradable basket into the high-trade-cost category.[17]

For the remaining parameters, we set $\nu^c = 3$ and $\nu^q = 3$. In our model, these parameters influence the price level, as shown in equation (14) through γ^x.[18] A higher ν^x, provided the condition $\nu^x < 1 + \theta^x$ is met, results in a lower price level. As long as this constraint is satisfied, the specific values of ν^c and ν^q are not critical, as they primarily serve to rescale the productivity vectors T^x_ℓ.

We want to estimate the parameters $(\alpha^f, \underline{c}^f)$. Our goal is, given prices and income, pick $(\alpha^f, \underline{c}^f)$ to describe the food expenditure shares as best as possible. Concretely, the estimated parameters solve

$$\widehat{(\alpha^f, \underline{c}^f)} \in \arg\min \left[\sum_i \sum_\ell \Lambda_{i,\ell} \left(s^{f,\text{data}}_{i,\ell} - s^{f,\text{model}}_{i,\ell}(\alpha^f, \underline{c}^f) \right)^2 \right]$$

[17] If we only considered food goods, excluding services, the shares would be $\alpha^c = 0.70$ and $\alpha^q = 0.30$.

[18] As in Eaton and Kortum (2002), these parameters must satisfy $\nu^x < 1 + \theta^x$ to ensure that basket prices are well-defined.

where we weighted the deviations by the population shares in income decile i in state ℓ, $\Lambda_{i,\ell}$. As explained earlier, the income brackets are defined at the national level, so the within state population is not necessarily even across i. In addition, the average income for each bracket i is not even across the states. We use this heterogeneity to discipline the effective hours, $e_{i,j}$ as follows: together with the level of Z_j^o, we calibrate $e_{i,j}$ to match the income level for each bracket at each state, according to $y_{i,j} = e_{i,j} Z_j^o$.

Our data for the expenditure shares come from the latest Consumer Expenditure Survey[19], conducted between 2017 and 2018. The coverage for the survey is national, and the unit of aggregation is the household level. In total, 57 920 households were interviewed, aiming to be representative of 69 017 704 households nationwide. The average family size is 3.00 persons per household.

From the microdata, we recover three estimates that are useful for our purposes: (i) the population distribution, measured by the number of households in each state; (ii) the income distribution at each state; (iii) the food expenditure shares at each state given an income bracket. Let i denote an income decile and ℓ denote a state. We take the income distribution at the national level and define brackets based on their deciles. Then, we take the microdata conditional for each state and recover the number of families within the brackets, together with their average income within the bracket. This process retrieves a matrix $\Lambda_{i,\ell}$ with the share of families living in state ℓ with income decile i, relative to the number of families across the country, together with a matrix $\mathcal{Y}_{i,\ell}$ with the average income under bracket i in state ℓ. We sum all expenditures and income for a given pair (i,ℓ) and take their ratio to recover the expenditure shares on a particular good type.

Calibration and Fit. The outcome of our estimation is $\alpha^f = 0.1694$, $\underline{c}^f = 0.0321$. The calibration approach mechanically gives more weight to the fit for states that have relatively more households, because $\Lambda_{i,\ell}$ for such states is higher. One alternative weighting scheme for this loss function is to attribute the same weight for the states, by setting an alternative weight that give the same weight for each bin (i,ℓ) in the loss function. The resulting parameters are qualitatively and quantitatively alike.

[19] Pesquisa de Orçamentos Familiares, POF, in Portuguese. The two other more recent versions are from 2008-2009 and 2002-2003.

Figure 2: Food Expenditure Share Across the Income Distribution

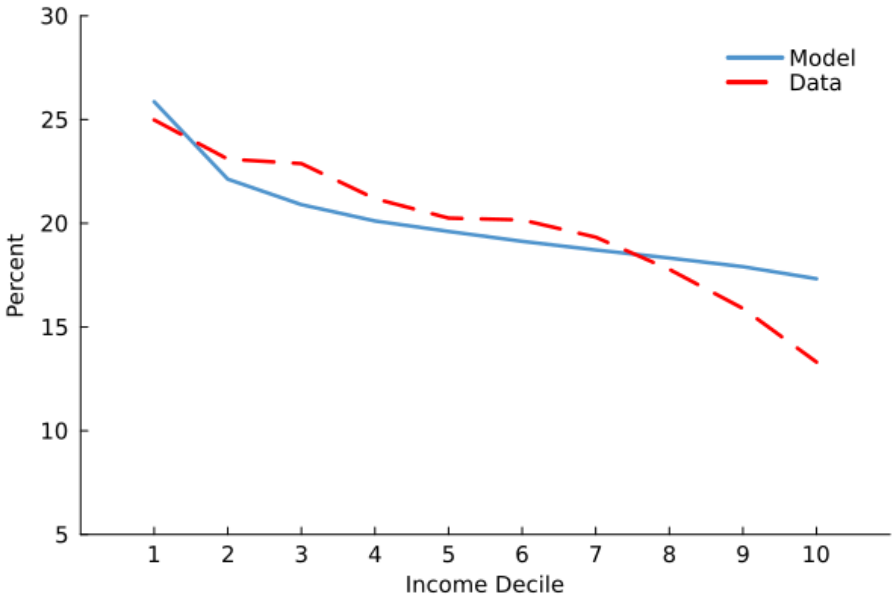

Notes: The figure shows the relationship between food expenditure shares and income deciles, comparing the model's predictions (blue solid line) with the actual data (red dashed line). The y-axis represents the percentage of total expenditure allocated to food, while the x-axis corresponds to income deciles, from the lowest (1st decile) to the highest (10th decile).

The model fit, with the food expenditure share at the national level, is shown in Figure 2. Figure illustrates the relationship between food expenditure shares and income deciles, comparing model predictions with actual data. The y-axis represents the percentage of total expenditure allocated to food, while the x-axis displays income deciles, ranging from the lowest (1st decile) to the highest (10th decile). As income increases, the food expenditure share tends to decline, in the data and in the model. In the model, the decline is tied to the decrease in $\psi^f_{i,\ell}$ as increase increase. This variable captures the cost of the floor consumption of food relative to total income. The severity of this cost depends on the state, as the price of food is dispersed across space due to the trade frictions.

The model provides a close fit to the actual data, particularly in the lower and middle-income deciles, where the predicted and observed shares are closely aligned. However, there is a slight divergence in the higher income deciles, where the model underestimates the share of expenditure on food compared to the observed data. Alternative specifications for the out-layer of the utility functions, e.g. Comin et al. (2021) might help improve the fit for the upper income deciles[20].

[20]This is work in progress.

Table 4: Model parameters under the benchmark calibration

Parameter		Value	Source
Productivity			
T_ℓ^x	State of Technology	[†]	Average potential productivity, section 4.4
Z_ℓ^o	Outside Good Productivity	[†]	Household labor survey, section 4.4
Trade			
$\tau_{j,\ell}^x$	Trade Frictions	[‡]	Specification in Equation 31
δ^c	Trade cost elasticity, LTC	0.30	Regression of price on heat shocks, section 4.4
δ^q	Trade cost elasticity, HTC	0.56	Regression of price on heat shocks, section 4.4
θ^x	Trade elasticity for LTC and HTC	3.39	Literature, section 4.4
Preferences			
α^f	Food weight in utility function	0.16	Joint estimation for $\boldsymbol{p} \equiv (\alpha^f, \underline{c}^f)$, section 5.2
$\underline{c}^f$	Minimum consumption of food	0.03	Joint estimation for $\boldsymbol{p} \equiv (\alpha^f, \underline{c}^f)$, section 5.2
ν^c	Elasticity of Substitution across LTC food	3.00	Normalization of Price level, section 5.2
ν^q	Elasticity of Substitution across HTC food	3.00	Normalization of Price level, section 5.2
α^c	LTC expenditure share within food	0.50	Consumer Prince Index basket, section 5.2
α^q	HTC expenditure share within food	0.50	Consumer Prince Index basket, section 5.2
Distributions: Population and Income			
$\Lambda_{i,\ell}$	Population shares under income i in location ℓ	[‡]	Consumer Expenditure Survey, section 5.2
$\mathcal{Y}_{i,\ell}$	Income level for location	[‡]	Consumer Expenditure Survey, section 5.2

Notes: [†] refers to either a vector of values, while [‡] refers to a matrix of values.

As the authors explain, the drawback with the Stone-Geary formulation is that when income is high, the subsistence cost becomes negligible, flattening the Engel curve. Extending the analysis in order to incorporate the Comin et al. (2021) preferences is relatively straight-forward because of the separation between the pricing of goods and the income.

Table 4 summarizes all the parameters for the calibration of the baseline, using the benchmark calibration.

6 Counterfactuals

With the baseline parameters established for the model, we proceed to outline the two counterfactual analyses we conduct. The first analysis explores how climate change impacts different regions and varies across income levels, focusing on changes in food prices. To assess this, we employed GAEZ projections under different scenarios for potential productivity concerning each food type x. The second analysis examines how enhancing transportation infrastructure in Brazil might reduce

the negative impacts of climate change by decreasing trade expenses.

6.1 Climate Change

In order to shed light on the main ingredients for our counterfactuals, we rewrite the equivalent variation formula, as in equation (23):

$$\mathrm{EV}_{i,j} = \sum_{x \in \mathcal{X}} \mathrm{s}^{x}_{i,j} \sum_{\ell \in \mathcal{L}} \pi^{x}_{j,\ell} \widehat{\mu}^{x}_{\ell}$$

In our model, we derive $s^x_{i,j}$ and $\pi^x_{j,\ell}$, and use $\hat{\mu}^x_\ell$ directly from the data. Alternatively, the expenditure shares $s^x_{i,j}$ can also be extracted directly from the Consumer Expenditure Survey microdata, offering more precise estimates by closely matching the actual data.[21] We determine the percentage change $\hat{\mu}^x_\ell$ by using the same methodology for calculating trade shares and determining T^x_ℓ, as detailed in subsection 4.4.1.

Our initial parameters include values for μ^x_ℓ, which we convert into values for T^x_ℓ. To determine the counterfactual value for these terms, we conduct the same procedures used to estimate T^x_ℓ in the baseline scenario, as outlined in section 4.4. The main distinction is that we now incorporate FAO projections for the potential yield of each crop under different Climate Change scenarios, replacing historical potential levels.

The procedure we undertake comprises the following steps. Initially, for each crop and location, we consider a set of counterfactual potential productivities. We perform two adjustments similar to those used to derive the metric μ^x_ℓ in the historical baseline scenario. First, land productivity is transformed into labor productivity using the input requirements from the most recent agricultural census. Following this, labor productivity is converted into a standardized unit by multiplying it by average historical prices. Ultimately, this provides a measurement of units of local currency per worker. For both adjustments, national averages are employed as a benchmark to minimize any interaction between trade frictions and revenue productivity, which could occur if location-specific input requirements and historical prices were used.

In an alternative scenario, $\mu^{x\prime}_\ell$ is defined as the average of this revenue productivity, serving as our measure for μ^x_ℓ. From the construction in equation (17), a corresponding State of Technologies

[21] We are currently recovering exact shares from the microdata directly.

vector, represented by $(T_\ell^x)'$, is derived to allow for the complete re-computation of the model. This lets us compare the results with those of the first-order method. For the results of the first-order approach, the logarithmic variations in μ_ℓ^x are used, which are determined by

$$\hat{\mu}_\ell^x \equiv \log(\mu_\ell^{x\prime}) - \log(\mu_\ell^x) \tag{38}$$

Importantly, similar to the approach in Costinot et al. (2016), in which the productivity of the outside sector is maintained constant, we assume that climate change does not influence productivity in the outside sector. If it did, an additional component would appear in the equivalent variation formula, as shown in equation (23), to account for changes in income. Although broadening the analysis within the model is straightforward, addressing the measurement concerns about changes in non-agricultural productivity is itself challenging, as noted in some strands of the literature (Bilal and Känzig, 2024; Bilal and Rossi-Hansberg, 2023; Cruz and Rossi-Hansberg, 2024). We proceed with a discussion of the data relevant to these hypothetical climate change scenarios.

6.2 Climate Change Scenarios

The GAEZ dataset offers numerous alternative forecasts for global crop potential productivity under various scenarios, presented as rasters. To determine potential productivities per state, we convert the raster data to align with state boundaries, yielding area-weighted potential productivity for each crop under each scenario, exactly as we did for the baseline model.

Apart from the assumptions regarding input intensity and irrigation practices, each scenario is characterized by three critical dimensions: the forecast timeline, the intensity of greenhouse gases responsible for warming, and the model that translates greenhouse gases concentration and other socioeconomic assumptions into temperature increases. We employed the high-input (maximum yield assumption with modern machinery) and rain-fed settings from the GAEZ portal. Costinot et al. (2016) uses this same high-input, rain-fed setup based on an earlier version (v3) of the GAEZ dataset.

Time Horizon. The first dimension concerns the time horizon. The GAEZ data set shows the historical potential productivity from 1981 to 2010[22]. The alternative scenarios present data for three 30-year periods, each with a point estimate. For these intervals — 2010-2040, 2041-2070, and 2071-2100 —– the reported crop potential yields are the simple average across the series, subject to all settings except time.

Greenhouse Gas Concentration. The second dimension considers future greenhouse gas concentrations under each scenario. Various assumptions correspond to distinct *Representative Concentration Pathways* (RCPs), as defined by the Intergovernmental Panel on Climate Change (IPCC) (Gutiérrez et al., 2021). These pathways are characterized by their radiative forcing levels, expressed in W/m^2. Four main trajectories include RCP 2.6, 4.5, 6.0, and 8.5. Generally, a lower value indicates a cooler Earth (less greenhouse forcing) and demands more stringent mitigation efforts to maintain that scenario.

Climate Models. The GAEZ offers crop potential yields derived from five distinct climate models, integrating RCPs as input[23]. For our analysis, we utilized the average yield from these models for each time frame (2040, 2070, 2100) and RCP (2.6, 4.5, 6.0, 8.5). These averages are applied at the crop level to determine the counterfactual average productivity, $\mu_\ell^{x\prime}$.

Summary. There are 60 triplet assortments, composed of three time horizons, four RCPs, and five climate models. Initially, we fix a time horizon and an RCP and then average potential crop yields over the climate models, reducing combinations to 12. Due to higher uncertainty in longer horizon estimates, our analysis concentrates on the 2040 time horizon and the optimistic scenario (RCP 2.6) concerning greenhouse gas concentrations. The choice for this Optimistic scenario is illustrative. Even for the lowest greenhouse gases contraction, there is already wide variability in the changes in productivity.

[22] 2010 marks the most recent year of available historical data. The project compiles several data sources to make these historical evaluations and forecasts, including temperature, precipitation, wind, and soil characteristics.

[23] The models include GFDL-ESM2m, HadGEM2-ES, IPSL-CM5A-LR, MIROC-ESM-CHEM, and NorESM1-M.

6.2.1 Details on the Productivity Changes

Significant variability exists in the percentage change of potential yield over short timescales among different crops and regions. Figure 3 illustrates this heterogeneity by depicting the change in *potential* yield under the Optimistic scenario for wetland rice in panel (a), cassava in panel (b), soybean in panel (c), and beans in panel (d) by 2040.

Rice yields drop by more than 20% in certain states. In contrast, cassava yields may increase by up to 15% in some southern areas, while others might see reductions over 10%. This divergence is rooted in the distinct needs for temperature, humidity, wind, soil, and terrain among crops, indicating that productivity changes result from factors beyond just a warming climate.

Figure 3 illustrates the diverse shifts in crop productivity across different regions. Our model requires an estimate of the average potential productivity for each food type, denoted as μ_ℓ^x. As outlined in section 4.4.1, and using the baseline productivity data, we determine the counterfactual values for μ_ℓ^x. With equation (38), we calculate the log change in this potential productivity and apply the equivalent variation formula from Equation (23).

Prior to examining the effects of productivity changes, we present the counterfactual measures μ_ℓ^x for various food types and regions. Figure 4 illustrates the smoothed histogram of these variations, highlighting two notable observations. There is notable variability across states for a given food type. The range of variation is around 40 percentage points: from -40% to 0% for HTC and -20% to 20% for LTC. Additionally, the distribution for HTC items skews more leftward. On average, the decline in productivity is more pronounced than that of LTC. Figure 5 illustrates the geographic spread of these productivity shifts, in two maps.

Figure 3: Percent Change in Yields, Optimistic Scenario, 2040

(a) Wetland Rice

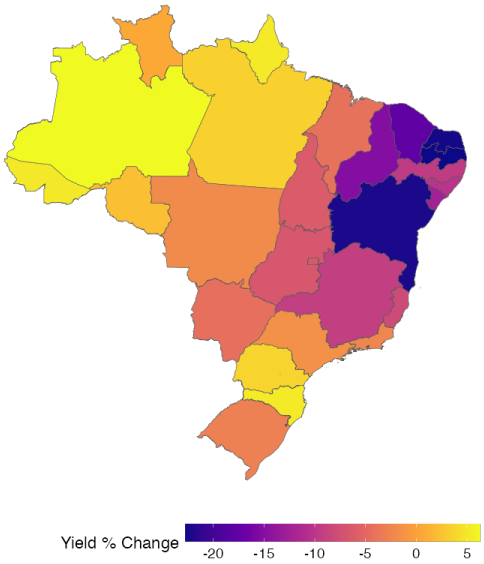

(b) Cassava

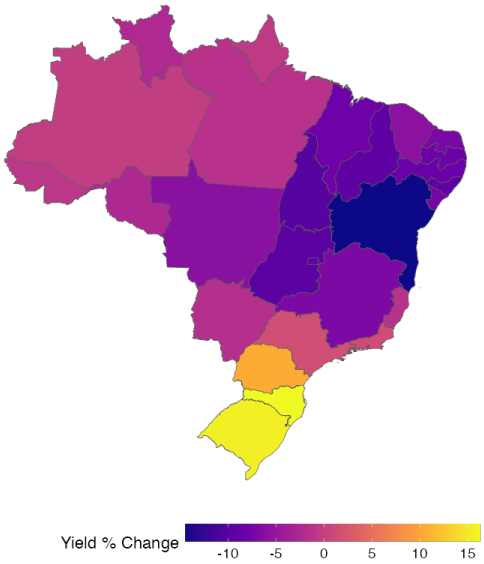

(c) Soybean

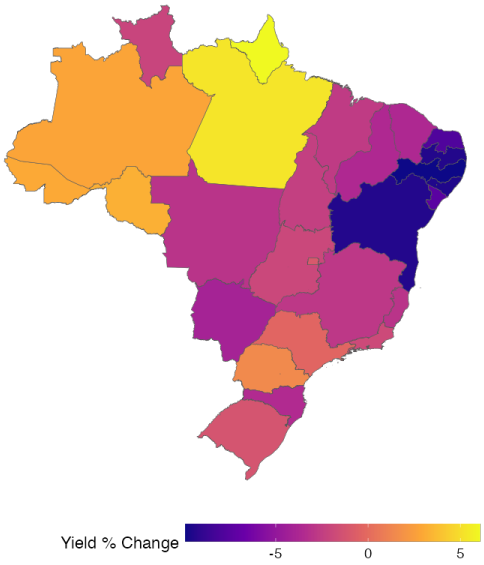

(d) Beans

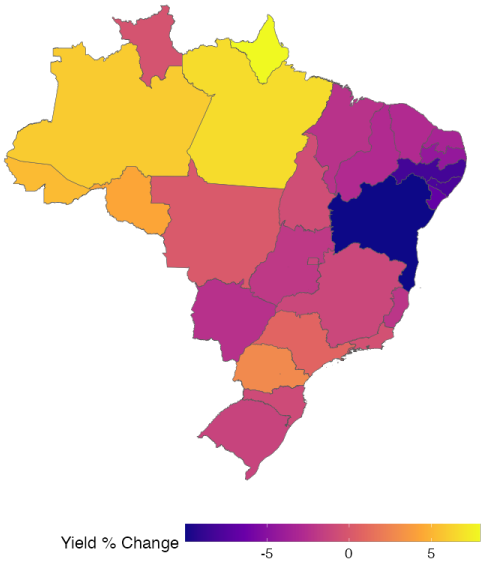

Notes: The maps illustrate the percentage shift in potential yield for Wetland Rice, Cassava, Soybean, and Beans, represented in panels (a), (b), (c), and (d), respectively, by 2040 under the Optimistic scenario (RCP 2.6). The counterfactual yield is based on the average from five climate models, as described in section 6.2. Though the heatmaps use similar color scales, they are not directly comparable; darker hues signify yield reductions, while warmer hues indicate yield increases. In this analysis, rice and soybean are classified as low-trade-cost foods, whereas beans and cassava fall into the high-trade-cost category.

Figure 4: Log change in μ_ℓ^x across the states, Optimistic Scenario, 2040.

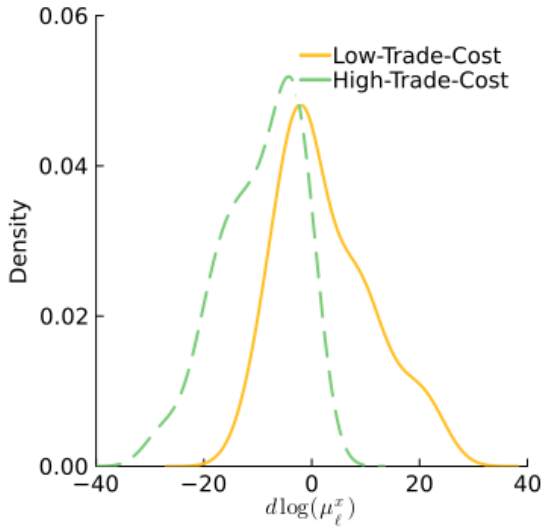

Notes: The figure shows the kernel density estimate for the log changes in the expected productivity of the food sectors, indexed by x, across the states. The change is given as equation (38), relative to the historical counterpart of the appropriate object.

6.2.2 Equivalent Variation

Upon obtaining the variations in average *potential* productivities, we apply the equivalent variation formula, as in equation (23). For households residing in a specific location j, the trade shares between states, $\pi_{j,\ell}^x$, and alterations in average potential productivities, $\hat{\mu}_\ell^x$, remain constant. The heterogeneity of outcomes within the region, due to productivity changes, is attributed to disparities in the food expenditure share, $s_{i,j}^x$, with the lowest income deciles being relatively more exposed.

Figure 6a presents the findings for the lowest income decile across states, focusing on this group due to its highest food expenditure share within each state. The central insight is related to productivity changes illustrated in Figure 4. Since productivity shifts in HTC goods are predominantly negative, their impact is adverse. Conversely, LTC productivity changes are approximately centered around zero. With minor trade costs, states engage more in LTC goods trading, making them more susceptible to inter-state changes. As a result, LTC contributions are less significant than HTC, and, for some states, even positive. We examine the impact of local productivity on the results, especially noting that the primary influence appears to be the goods facing high trade costs. Figure 7 depicts the relationship between the equivalent variation for the lowest income decile and

Figure 5: Percent Change in Average Potential Productivity, $\hat{\mu}_{\ell}^{x}$, Optimistic Scenario, 2040

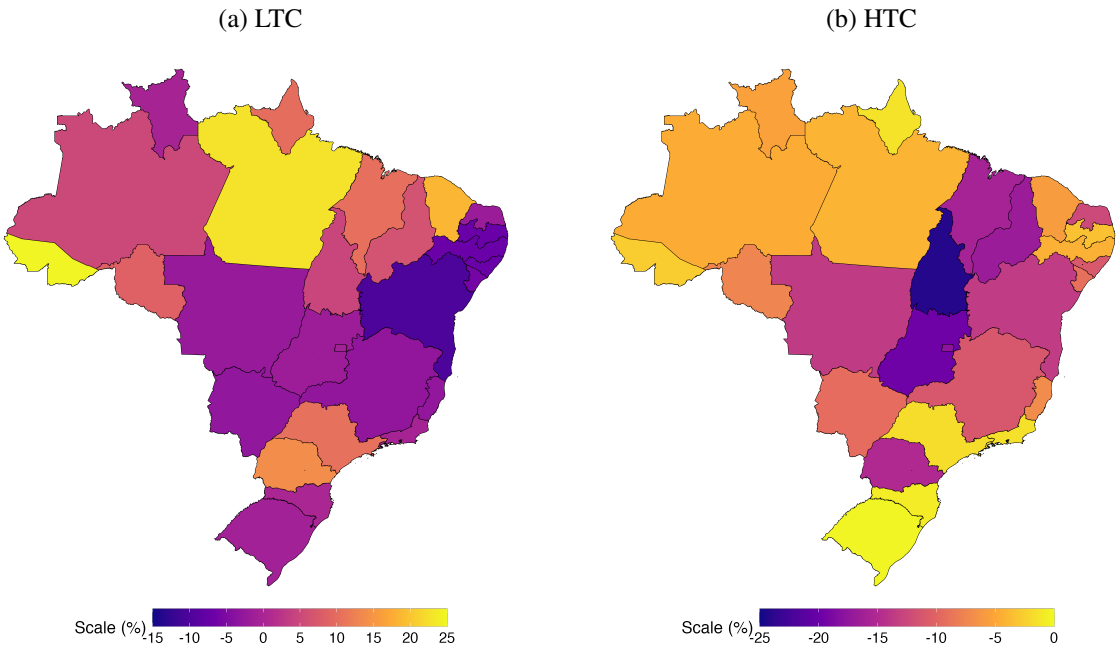

Note: The maps present the percentage change in average potential yield, μ_{ℓ}^{x}, compared to historical data for each state: panel (a) for LTC and panel (b) for HTC. This is projected for 2040 under the Optimistic scenario, RCP 2.6. The counterfactual yields represent the average from five climate models, detailed in section 6.2. Note that the heatmap color scales differ.

the variation in productivity for HTC food goods. For these goods, the trade costs are sufficiently high that $\pi_{j,\ell}^{x}$ approaches zero when $j \neq \ell$. Consequently, in equation (23), HTC's contribution arises mainly from changes in productivity within the same region, resulting in the marked correlation seen in figure 7.

Figure 6: Equivalent Variation across the states, Optimistic Scenario, 2040

(a) First income decile

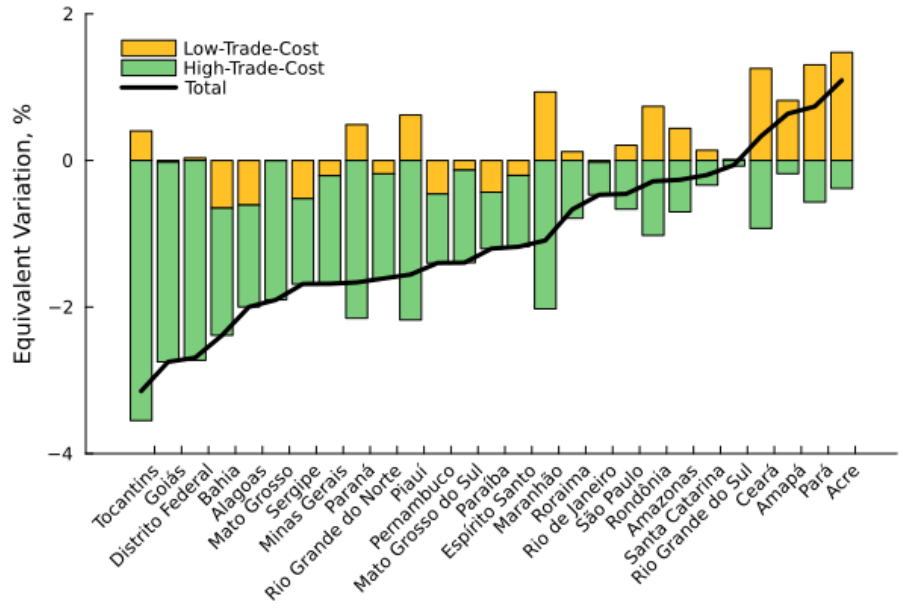

(b) Last income decile

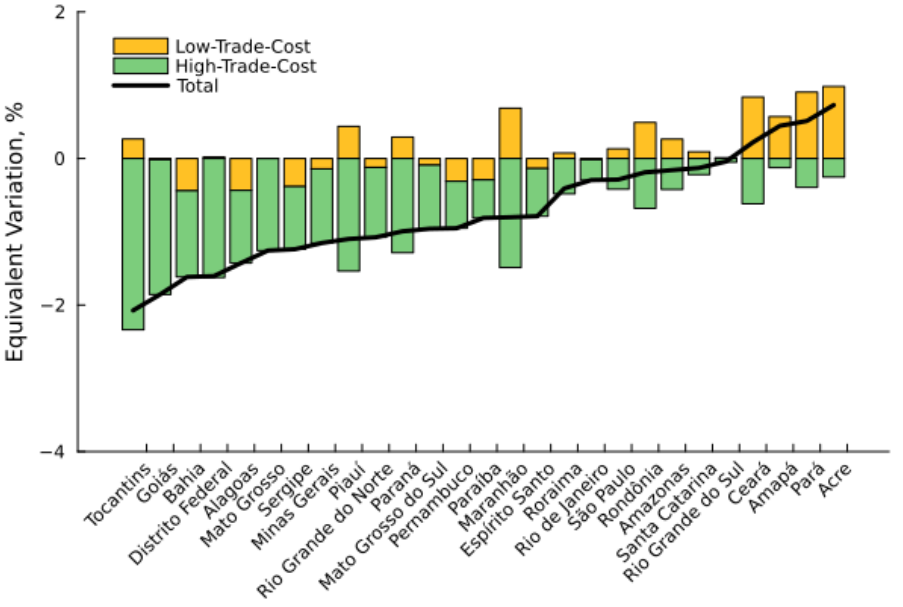

Note: The figures illustrate the equivalent variation for the lowest income decile, in panel (a), and the highest income decile, in panel (b). Green bars represent the HTC food goods contribution, whereas yellow bars indicate the LTC contribution. States are arranged from left to right, from the most adverse to the least adverse total change. Notice that, due to differences in the burden of subsistence ratio, per equation (36), associated with the local food price, the ordering of the states is not the same in both figures.

Figure 7: Equivalent Variation and change in HTC productivity

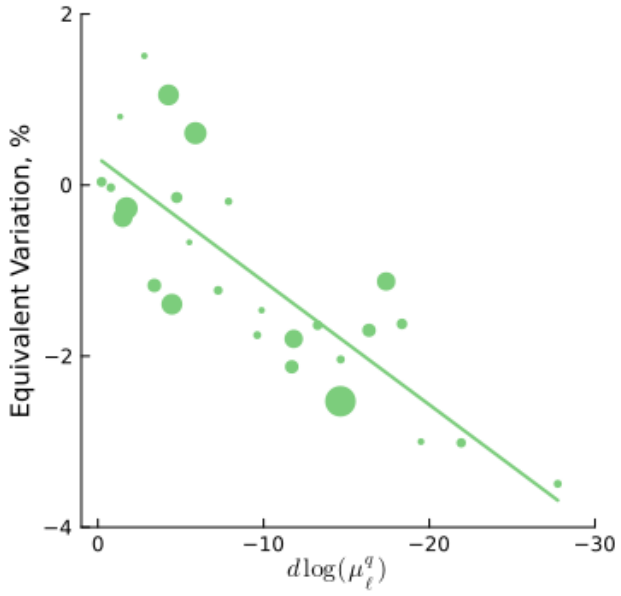

Notes: The figure displays a scatter plot illustrating the equivalent variation for the first decile in different states against changes in productivity for HTC food goods. The x-axis is reversed, indicating a decrease in productivity as one moves from left to right. Bubble size corresponds to population shares.

Figure 6b shows the counterpart of the equivalent variation for the highest-income decile. Notice that because of dispersion in the food price and in the income at the top of the distribution across states, the ordering of the states is not the same as in Figure 6a.

6.3 Improving the Roads

Next, we proceed to the second counterfactual analysis, which emphasises the role of roads in serving as a mitigation mechanism. We examine the structure applied to trade frictions, which are modeled based on driving time between states. Better road quality decreases these frictions, facilitating trade between locations. Consequently, reduced trade barriers enhance the adaptation mechanism for sourcing food goods. In Table 1 and the related text, we briefly described driving times between locations. Since the driving time between state capitals served as a proxy, the discussion was concise. Given the importance of driving time in this counterfactual analysis, we revisit the data.

Figure 8a presents a scatter plot illustrating driving distances (x-axis) versus driving times (y-axis) from three Brazilian state capitals, as detailed in Table 1. Distances and times are recorded in kilometers (km) and hours, respectively, with data points for each of the other 26 state capitals. Manaus, marked by red circles, is relatively isolated in the Amazon, averaging more than 1,000 kilometers from the nearest three capitals and often over 3,000 kilometers from many others. In contrast, Porto Alegre (green triangles) and São Paulo (blue squares) are closer to other capitals, resulting in shorter driving times. A best-fit line is included, showing average speeds as distance over time. For Manaus, this line is noticeably higher than those of Porto Alegre and São Paulo, indicating greater distances and reduced average speeds, as evidenced in Table 1.

Figure 8b provides an alternative perspective on average speed heterogeneity. This illustration includes the same three state capitals, but the y-axis now displays the average speed from each origin to all other state capitals. Notably, for Porto Alegre and São Paulo, the average speed remains relatively stable across distances, centered around 75 km/h, with fluctuations from approximately 65 to 80 km/h. São Paulo, being more centrally located, has numerous state capitals within a 3,000 km radius. In contrast, Manaus exhibits a consistently lower average speed across the distance range, with an observable increase in speed as the distance grows, highlighting low speeds *near*

Manaus. This suggests that considering distance can overlook the additional travel cost in areas with lower average speeds.

Figure 8: Alternative measures of driving frictions

(a) Driving Time, hours

(b) Average Speed, km per hour

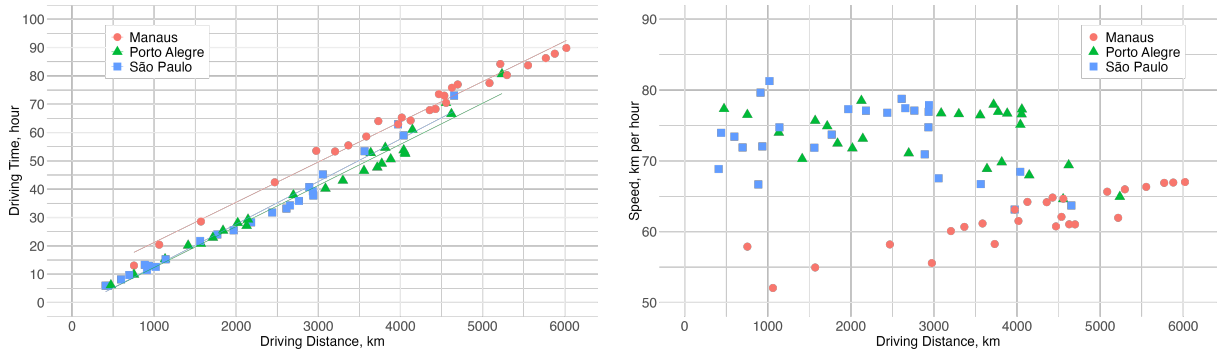

Notes: Two scatter plots are depicted, with Driving distance (km) on the horizontal axis versus two distinct driving metrics. Panel (a) presents driving time in hours, and panel (b) illustrates average speed in km/h. Each point represents data from one origin compared to all 26 Brazilian state capitals: Manaus (red, circles), Porto Alegre (green, triangles), and São Paulo (blue, squares). These origins correspond to those in Table 1.

Consider now our counterfactual scenario. Assume an increase in the average road speed by ϕ%. Since the trade friction is a constant elasticity function of driving time, the reduction in trade cost corresponds to this elasticity as follows:

$$\frac{\partial \log(\tau_{j,\ell}^{x})}{\partial \log(d_{i,j})} = \delta^{x} \tag{39}$$

assuming $j \neq \ell$. Consequently, a rise in average speed by ϕ% results in a trade cost adjustment of $-\phi\delta^{x}$. This reduction in trade barriers decreases price levels at each location according to:

$$\frac{\partial \log(P_{j}^{x})}{\partial \log(\tau_{j,\ell}^{x})} = \pi_{j,\ell}^{x} \tag{40}$$

The equivalent variation is

$$\begin{aligned} \mathrm{EV}_{i,j} &= \sum_{x\in\mathcal{X}} \mathrm{s}_{i,j}^{x} \sum_{\ell\neq j} \pi_{j,\ell}^{x} \delta^{x} \phi \\ &= \sum_{x\in\mathcal{X}} \mathrm{s}_{i,j}^{x} (1-\pi_{j,j}^{x}) \delta^{x} \phi \end{aligned} \tag{41}$$

The initial row acknowledges $\tau^x_{j,j} = 1$, while the final row considers that total trade shares equal 1. Equation (41) stresses the significance of the own-trade share, as discussed in Arkolakis et al. (2012). With given expenditure shares $s^x_{i,j}$ and elasticity δ^x, the own-trade share $\pi^x_{j,\ell}$ provides a sufficient metric for calculating equivalent variation to first-order.

The first-order method offers a streamlined formulation to separate each type of food's contribution to the equivalent variation. Although the elasticity of trade friction to driving time for high-trade-cost foods, δ^q, is double that for low-trade-cost foods, δ^c, typically the own-trade share is larger for high-trade-cost foods. These opposing factors introduce variability in the policy impacts.

Figure 9: Equivalent Variation from Road Improvement, first income decile,

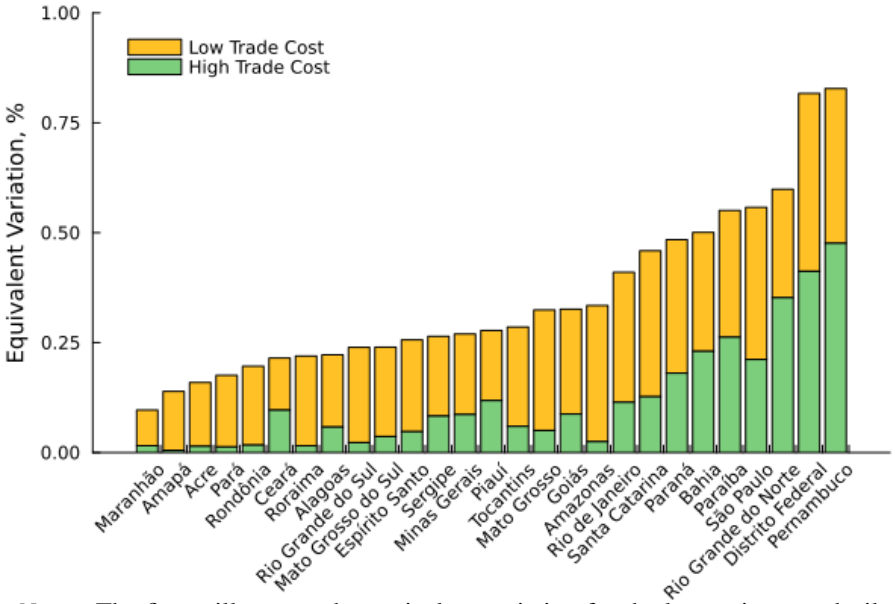

Notes: The figure illustrates the equivalent variation for the lowest income decile across states, following a 10% increase in average road speed post-climate change. The green indicates HTC food goods' impact, whereas the yellow represents LTC's contribution. States are arranged from left to right, from the worst to best total change.

7 Discussion and Potential Extensions

In this section, we discuss key assumptions and potential extensions of the model. While our framework focuses on the main forces of production and trade pattern shifts driven by new comparative advantages, it omits other adaptation margins, such as migration and the role of immobile

factors like land and housing.

Migration. Significant differences in productivity changes across states suggest that households might be less inclined to stay in regions likely to face reduced productivity, particularly if they are remote. By constraining migration in our model, we may overstate the adverse effects on these households. Barbosa-Alves and Britos (2023) highlights how financial frictions and declining productivity prospects influence migration. Our approach aligns with the baseline model of Ramondo et al. (2016), which excludes migration to focus on domestic trade frictions, a central element of our analysis.

Although our model does not predict migration flows, the relative productivity changes and their effects on utility across regions can indicate potential migration directions. For example, if a state like Tocantins is expected to face declining productivity, residents may consider relocating. The scale and economic impact of such migration is a quantitative question, and incorporating migration into the model would be a valuable extension for future research.

Lower transportation costs could also encourage migration. Recent studies show how reduced transport costs have spurred migration and enabled the exploration of new comparative advantages. For Brazil, Morten and Oliveira (2024) documents how the transport network developed around Brasília in the 1950s boosted both trade and internal migration. Similarly, Pellegrina and Sotelo (2024) attributes the "March to the West" in Brazil during the late 20th and early 21st centuries to improved road infrastructure, which arguably have lowered migration costs and shaped regional productivity. In a way, this argument connects to Donaldson and Hornbeck (2016), where the authors utilize the expansion of railroads in the late 19th-century United States as a means to investigate the revaluation of land due to surge in new comparative advantages.

Immobile Factors. As shifts in comparative advantage drive migration, immobile factors such as land and housing can limit these movements. For regions experiencing an outflow of residents, land and housing would become relatively abundant, potentially leading to a decline in their prices. This could deter further migration, as lower costs of living might encourage households to stay. Donaldson and Hornbeck (2016) illustrates how reduced trade barriers, through railway expansion in the late 19th century U.S., led to higher land values. A similar example is seen in Donaldson

(2018).

Incorporating land as an explicit production factor could further enhance the ability to test the goodness of fit of the model. This addition would allow for validation against land use patterns observed in the data, as explored in studies like Costinot et al. (2016), Sotelo (2020), and Pellegrina (2022). Our model implicitly assumes a Leontief production function between land and labor, where land is relatively abundant, making labor the binding constraint on food production.

Other Considerations. The actual price of food also reflects processing costs beyond raw agricultural products. Ignoring these costs may lead us to overstate the effects of declines in crop productivity on overall food prices. Additionally, we classify foods as either low-trade-cost (LTC) or high-trade-cost (HTC), but some goods, like animal products, may fall between these categories due to transportation needs such as refrigeration. While these products are included in the LTC group because of their classification as "tradables" by the Brazilian Central Bank, they may warrant separate analysis. Pellegrina (2022) finds that trade distance elasticities for cereals and "other non-perishable" foods, including beef, are similar. Further refining the model to incorporate a more detailed breakdown of consumer food costs would enhance our estimates.

8 Conclusion

In this paper, we developed a multi-location model of food production and trade to analyze the effects of climate change on food prices and income inequality. The framework incorporates heterogeneity in food tradability, location-specific productivity, regional connectivity, and income distribution within each location. We applied the model to Brazil, a country with significant geographical and climatic diversity, to examine how these factors interact to shape food prices and household welfare under climate change.

The results indicate that trade frictions play a central role in limiting regional adaptation to changes in local food productivity, particularly for goods with high trade costs. As climate change alters agricultural productivity, the limited adaptability of high-trade-cost goods underscores the importance of these trade frictions. This dynamic poses greater risks for poorer households, which allocate a larger share of their income to food and are therefore more susceptible to price increases.

Consequently, the uneven impacts of climate change on food prices have implications for existing income inequalities within and across regions.

Our counterfactual analysis suggests that reducing trade frictions through improvements in road infrastructure can serve as an adaptation strategy. Enhanced connectivity lowers trade costs, enabling regions to source food more efficiently from more productive areas, which helps mitigate local price pressures. This, in turn, can dampen adverse welfare effects, particularly for low-income households that are more exposed to food price increases. Although the findings are specific to Brazil, the mechanisms and methods developed here can be applied to other regions with similar vulnerabilities, such as India or parts of Africa, where climate change and transportation infrastructure constraints are also pertinent issues.

While the model emphasizes trade frictions, it abstracts from other adaptation strategies that may also be significant. For example, migration between regions could serve as a response to changes in local productivity. Although migration flows are not estimated, differences in cross-state effects from the equivalent variation analysis offer insights into potential migration directions. Barbosa-Alves and Britos (2023) discusses how local changes in agricultural productivity can influence migration. Another relevant consideration is the valuation of fixed factors, such as land and housing. Extending the framework to include these factors could provide a more comprehensive understanding of the adaptation mechanisms and is a potential area for future research.

References

Adao, R., Costinot, A., and Donaldson, D. (2017). Nonparametric counterfactual predictions in neoclassical models of international trade. *American Economic Review*, 107(3):633–689.

Agnosteva, D. E., Anderson, J. E., and Yotov, Y. V. (2014). Intra-national trade costs: Measurement and aggregation. Technical report, National Bureau of Economic Research.

Albert, C., Bustos, P., and Ponticelli, J. (2024). The effects of climate change on labor and capital reallocation. *Unpublished manuscript*.

Allen, T. and Atkin, D. (2022). Volatility and the gains from trade. *Econometrica*, 90(5):2053–2092.

Arkolakis, C., Costinot, A., and Rodríguez-Clare, A. (2012). New trade models, same old gains? *American Economic Review*, 102(1):94–130.

Astorga-Rojas, D. (2024). Access to markets and technology adoption in the agricultural sector: Evidence from brazil. *Unpublished manuscript*.

Asturias, J., García-Santana, M., and Ramos, R. (2019). Competition and the welfare gains from transportation infrastructure: Evidence from the golden quadrilateral of india. *Journal of the European Economic Association*, 17(6):1881–1940.

Atkin, D. and Donaldson, D. (2015). Who's getting globalized?: The size and implications of intra-national trade costs. (w21439).

Auer, R., Burstein, A., Lein, S. M., and Vogel, J. (2022). Unequal expenditure switching: Evidence from switzerland. Technical report, National Bureau of Economic Research.

Barbosa-Alves, M. and Britos, B. (2023). Climate change and international migration.

Bilal, A. and Känzig, D. R. (2024). The macroeconomic impact of climate change: Global vs. local temperature. Technical report, National Bureau of Economic Research.

Bilal, A. and Rossi-Hansberg, E. (2023). Anticipating climate change across the united states. Working Paper 31323, National Bureau of Economic Research.

Brazilian Central Bank (2019). Ipca weighting structure updates and repercussions in its classifications. Box, Brazilian Central Bank. Available at: https://www.bcb.gov.br/content/ri/inflationreport/201912/ri201912b7i.pdf.

Castro-Vincenzi, J., Khanna, G., Morales, N., and Pandalai-Nayar, N. (2024). Weathering the storm: Supply chains and climate risk. Technical report, National Bureau of Economic Research.

Comin, D., Lashkari, D., and Mestieri, M. (2021). Structural change with long-run income and price effects. *Econometrica*, 89(1):311–374.

Copernicus Climate Change Service (2019). ERA5-Land hourly data from 2001 to present.

Costinot, A., Donaldson, D., and Smith, C. (2016). Evolving comparative advantage and the impact of climate change in agricultural markets: Evidence from 1.7 million fields around the world. *Journal of Political Economy*, 124(1):205–248.

Cruz, J.-L. and Rossi-Hansberg, E. (2024). The economic geography of global warming. *Review of Economic Studies*, 91(2):899–939.

Donaldson, D. (2018). Railroads of the raj: Estimating the impact of transportation infrastructure. *American Economic Review*, 108(4-5):899–934.

Donaldson, D. and Hornbeck, R. (2016). Railroads and american economic growth: A "market access" approach. *The Quarterly Journal of Economics*, 131(2):799–858.

Eaton, J. and Kortum, S. (2002). Technology, geography, and trade. *Econometrica*, 70(5):1741–1779.

Faccia, D., Parker, M., and Stracca, L. (2021). Feeling the heat: extreme temperatures and price stability.

Fajgelbaum, P. D. and Khandelwal, A. K. (2016). Measuring the unequal gains from trade. *The Quarterly Journal of Economics*, 131(3):1113–1180.

FAO and IIASA (2022). Global agro-ecological zones (gaez v4) - data portal. https://gaez.fao.org/. Accessed: 2024-10-16.

Fitzgerald, D. (2008). Can trade costs explain why exchange rate volatility does not feed into consumer prices? *Journal of monetary Economics*, 55(3):606–628.

Gutiérrez, J., Jones, R., Narisma, G., Alves, L., Amjad, M., Gorodetskaya, I., Grose, M., Klutse, N., Krakovska, S., Li, J., Martínez-Castro, D., Mearns, L., Mernild, S., Ngo-Duc, T., van den Hurk, B., and Yoon, J.-H. (2021). *Atlas*. Cambridge University Press. In Press. Interactive Atlas available from http://interactive-atlas.ipcc.ch/.

Morten, M. and Oliveira, J. (2024). The effects of roads on trade and migration: Evidence from a planned capital city. *American Economic Journal: Applied Economics*, 16(2):389–421.

Oni, M. H. (2024). Commuting, home utilities, and production: The distributional effect of energy price shocks. *Unpublished manuscript*.

Pellegrina, H. S. (2022). Trade, productivity, and the spatial organization of agriculture: Evidence from brazil. *Journal of Development Economics*, 156:102816.

Pellegrina, H. S. and Sotelo, S. (2024). Migration, specialization, and trade: Evidence from brazil's march to the west. *Journal of Political Economy (Forthcoming)*.

Ramondo, N., Rodríguez-Clare, A., and Saborío-Rodríguez, M. (2016). Trade, domestic frictions, and scale effects. *American Economic Review*, 106(10):3159–3184.

Schlenker, W. and Roberts, M. J. (2009). Nonlinear temperature effects indicate severe damages to us crop yields under climate change. *Proceedings of the National Academy of sciences*, 106(37):15594–15598.

Simonovska, I. and Waugh, M. E. (2014). The elasticity of trade: Estimates and evidence. *Journal of international Economics*, 92(1):34–50.

Somanathan, E., Somanathan, R., Sudarshan, A., and Tewari, M. (2021). The impact of temperature on productivity and labor supply: Evidence from indian manufacturing. *Journal of Political Economy*, 129(6):1797–1827.

Sotelo, S. (2020). Domestic trade frictions and agriculture. *Journal of Political Economy*, 128(7):2690–2738.

World Bank (2022). Brazil infrastructure assessment (p174544) synthesis report.

A Data

A.1 Exposure Data

Figure A.1 exhibits the temperature observed on a hypothetical day. The day starts at around $10^{\circ}C$ and ends at around $14^{\circ}C$. As the temperature rises, it eventually surpasses the threshold of $30^{\circ}C$ at around 8 a.m. and remains above this threshold until approximately 4:30 p.m., so the total exposure to $30^{\circ}C$ is $8.5/24 \approx 0.3541$ day. The temperature remains above $35^{\circ}C$ between 10:30 a.m. and 2 p.m., so the exposure to $35^{\circ}C$ is $3.5/24 \approx 0.1458$ day.

Figure A.1: Exposure to temperature thresholds

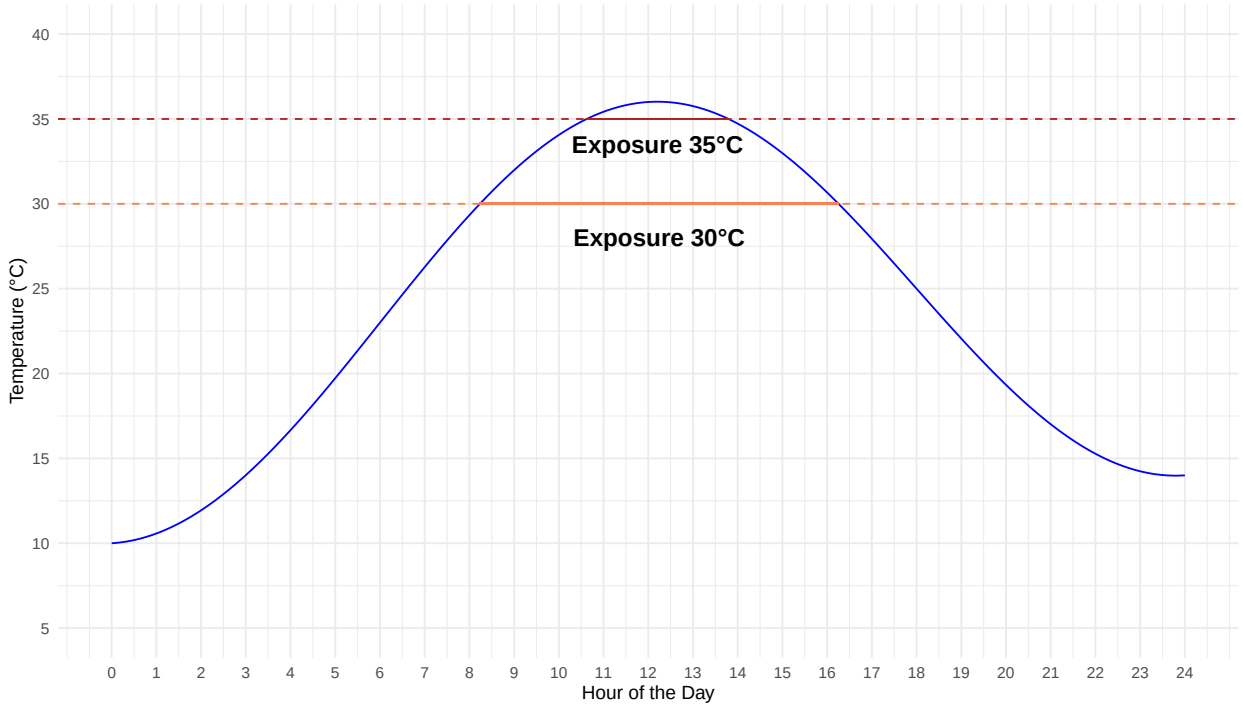

Notes: The figure illustrates the exposure to different temperature cutoffs throughout a hypothetical day.

Our weather data is hourly. We compute the exposure to different temperature thresholds for each municipality and month, combining the weather data and the official municipality boundaries from IBGE for the year 2022. We then aggregate it at the quarterly frequency.

Since the CPI data is available at the location level that is unique for each state, the regression uses the exposure measure at the state level. We first compute the exposure at the municipality

level and then weigh each municipality within the state by the crop production value as follows

$$\text{Heat}_{\ell,t} \equiv \sum_{l \in M_\ell} \text{Heat}_{l,t} \times \tilde{w}_{l,\ell} = \sum_{l \in M_\ell} \text{Heat}_{l,t} \times \left(\frac{w_{l,\ell}}{\sum_{l \in M_\ell} w_{l,\ell}} \right) \tag{1}$$

where M_ℓ is the set of all municipalities in state ℓ. The weight is $w_{l,\ell}$ for municipality l at state ℓ, and is given by

$$w_{l,\ell} = \sum_{y=1999}^{2021} \frac{\text{CPV}_{l,y}}{22} \tag{2}$$

where $\text{CPV}_{l,y}$ is the total crop production value. As we detail in Appendix A.2, the data for such series comes at annual frequency, at crop and municipality level. The data starts in 1974 and finishes in 2021. We use the data from 1999 to be lined up as much as possible with the CPI coverage. Hence, $w_{l,\ell}$ is the time average crop production value at the municipality l. This weight is time-invariant throughout the sample.

A.2 Crop Production Data

We use the Systematic Survey of Agricultural Production[24] from IBGE as the main source for crop production data. Our data comes in annual frequency and provides the value of production, planted area, harvest area, quantity produced, and average yield at the level of crop and municipality. We refer to appendix A.2 for a detailed list of crops that are covered.

The data covers the years 1974 to 2021. We use the production value data to weigh the observations (municipalities) around a reference city for the metro area when constructing the exposure measure we use to run the regression in (32). Specifically, we first compute the exposure to a given threshold of temperature for each municipality at the monthly frequency. Then, for each metro area in our CPI data, we consider all cities that are within the state limits for that metro area. The measure of exposure for each metro area is the weighted average of exposure of all municipalities within the state boundaries, and the relative weight is given by the total (nominal) crop production value, averaged from 1999 to 2021, to overlap with our CPI data coverage, as much as possible.

A.2.1 Link between Heat Exposure and Crop Yields

We use a long panel of data to examine the relationship between heat exposure and crop yields. Our findings show that temperatures exceeding $30^{\circ}C$ tend to reduce crop yields, consistent with Schlenker and Roberts (2009) based on U.S. data. We estimate this effect using a panel regression where the dependent variable is yield, regressed on heat exposure at a specified cutoff, T. As in the main text, we set $T = 30^{\circ}C$. Heat exposure is measured during the crop season, defined from September to May, which covers the most significant crops in terms of production value that share a common or overlapping growing period.

$$\log(\text{yield}_{\ell,t}) = \beta_0 + \beta_h \text{Heat}_{t,\ell} + \mathbf{\Gamma} \boldsymbol{X}_{\ell,t} + \alpha_\ell + \alpha_t + \epsilon_{\ell,t} \tag{3}$$

Here, t represents time, and ℓ denotes location. The variable $\text{Heat}_{t,\ell}$ measures exposure above the temperature of $30^{\circ}C$. We include location fixed effects to control for time-invariant, location-specific factors, and time fixed effects to account for aggregate shocks. The vector $\boldsymbol{X}t,\ell$ comprises additional controls for robustness checks, including state and regional trends, as well as interactions

[24] In Portuguese, "Levantamento Sistemático da Produção Agrícola".

of states and regions with years.

For brevity, we show three regressions here. The crops for these regressions are rice, soybean, and beans. Rice and soybeans are classified as "tradable" in the Brazilian Central Bank CPI classification, while beans are classified as "non-tradable". Again, "tradable" refers to our low-trade-cost, LTC, and "non-tradable" refers to our high-trade-cost, HTC. We ran one regression separately per crop to allow the fixed effect to control for crop-specific forces at locations and aggregate effects. Alternatively, one could interact with each fixed effect with a crop dummy together with the exposure variable.

The coefficient β_h is a semi-elasticity. For example, one additional day of exposure above $30^{\circ}C$ during the crop season decreases the rice yield by 0.40% and the beans yield by 0.6%, after controlling for state-year fixed effects.

Table A.1: Regression (3) results: Rice

	Dependent variable: $100 \times \log(\text{yield}_{t,\ell})$				
	(1)	(2)	(3)	(4)	(5)
$\text{Heat}_{t,\ell}$	-1.40***	-1.37***	-0.795***	-1.41***	-0.392***
	(0.0512)	(0.0494)	(0.0519)	(0.0471)	(0.0554)
Observations	154501	154501	154501	154501	154501
R-squared	0.172	0.185	0.273	0.198	0.376
Number of Municipalities	4837	4837	4837	4837	4837
Municipality FE	✓	✓	✓	✓	✓
Year FE	✓	✓	✓	✓	✓
Regional Trend		✓			
Regional Dummy x Year			✓		
State Trend				✓	
State Dummy x Year					✓

Note: This table shows the results of regression (3), with several controls. Robust standard errors are in parentheses. *** p<0.01, ** p<0.05, * p<0.1. All regressions include both Municipality and Year Fixed Effects. The regression in Column (1) does not include any other controls. Column (2) adds the control for the Regional Trend. Column (3) adds an interaction of a Regional Dummy with Year. Column (4) adds a State Trend. Column (5) adds an interaction between a State Dummy and Year.

Table A.2: Regression (3) results: Soybean

	Dependent variable: $100 \times \log(\text{yield}_{t,\ell})$				
	(1)	(2)	(3)	(4)	(5)
$\text{Heat}_{t,\ell}$	-0.951***	-1.05***	-0.891***	-0.951***	-0.599***
	(0.0345)	(0.0362)	(0.0382)	(0.0365)	(0.00037)
Observations	73240	73240	73240	73240	73240
R-squared	0.508	0.51	0.583	0.522	0.66
Number of Municipalities	2881	2881	2881	2881	2881
Municipality FE	✓	✓	✓	✓	✓
Year FE	✓	✓	✓	✓	✓
Regional Trend		✓			
Regional Dummy x Year			✓		
State Trend				✓	
State Dummy x Year					✓

Note: This table shows the results of regression (3), with several controls. Robust standard errors are in parentheses. *** p<0.01, ** p<0.05, * p<0.1. All regressions include both Municipality and Year Fixed Effects. The regression in Column (1) does not include any other controls. Column (2) adds the control for the Regional Trend. Column (3) adds an interaction of a Regional Dummy with Year. Column (4) adds a State Trend. Column (5) adds an interaction between a State Dummy and Year.

Table A.3: Regression (3) results: Beans

	Dependent variable: $100 \times \log(\text{yield}_{t,\ell})$				
	(1)	(2)	(3)	(4)	(5)
$\text{Heat}_{t,\ell}$	-1.04***	-0.895***	-0.721***	-0.941***	-0.604***
	(0.0372)	(0.0345)	(0.0363)	(0.0341)	(0.0404)
Observations	207222	207222	207222	207222	207222
R-squared	0.172	0.217	0.269	0.24	0.371
Number of Municipalities	5522	5522	5522	5522	5522
Municipality FE	✓	✓	✓	✓	✓
Year FE	✓	✓	✓	✓	✓
Regional Trend		✓			
Regional Dummy x Year			✓		
State Trend				✓	
State Dummy x Year					✓

Note: This table shows the results of regression (3), with several controls. Robust standard errors are in parentheses. *** p<0.01, ** p<0.05, * p<0.1. All regressions include both Municipality and Year Fixed Effects. The regression in Column (1) does not include any other controls. Column (2) adds the control for the Regional Trend. Column (3) adds an interaction of a Regional Dummy with Year. Column (4) adds a State Trend. Column (5) adds an interaction between a State Dummy and Year.

A.3 CPI Data — Additional Details

A.3.1 Locations and Broad Baskets

Table A.4 reveals details for the locations we consider in the analysis. There are 16 locations in the panel, most of which are metro areas. All the locations that are labeled as "municipality" are the state capital. For each state, there is at most one location, but not all states are covered by the CPI data, as figure A.2 shows. Out of 27 states, 16 are currently tracked in the CPI data, either by its capital or the metroarea that include its capital.

The weight of each location when constructing the national index is highly variable, as the column "Location" highlights. Locations with high total household income receive higher weights, conditioning on income from 1 to 40 minimum wages. For example, the location of "São Paulo" has the highest weight because it is the most populated state in Brazil and has a relatively high household income[25]. These location weights are not used directly in our estimation.

The table shows the weight in the CPI basket for Food overall and breaks down these weights into "Tradable" and "Nontradable" according to the Central Bank Classification exposed in A.4. The range for the weight of Food in the basket is 26.6 percent to 16.8 percent.

The table also illuminates regional differences in the consumption basket. Locations with lower weight are usually poorer and tend to have a relatively high expenditure share on Food. On the other hand, locations with higher weights tend to consume a relatively larger share of Nontradable food within the group "Food". The reason is that the "Food" group contains subitems related to services, such as eating out, which tend to be a relatively larger share of the expenditure as income increases.

Figure A.2 brings a map of the state boundaries and the year when the locations associated with each state became available in our sample. The sample we consider starts in 1999, and by that year, there were already 11 locations in the CPI. In January 2014, Campo Grande (MS) and Vitória (ES) became covered. In May 2018, Rio Branco (AC), São Luis (MA), and Aracaju (SE) data became available.

[25] For brevity of the exposition, we omitted these two information from the table.

Figure A.2: Locations for which the CPI data is available

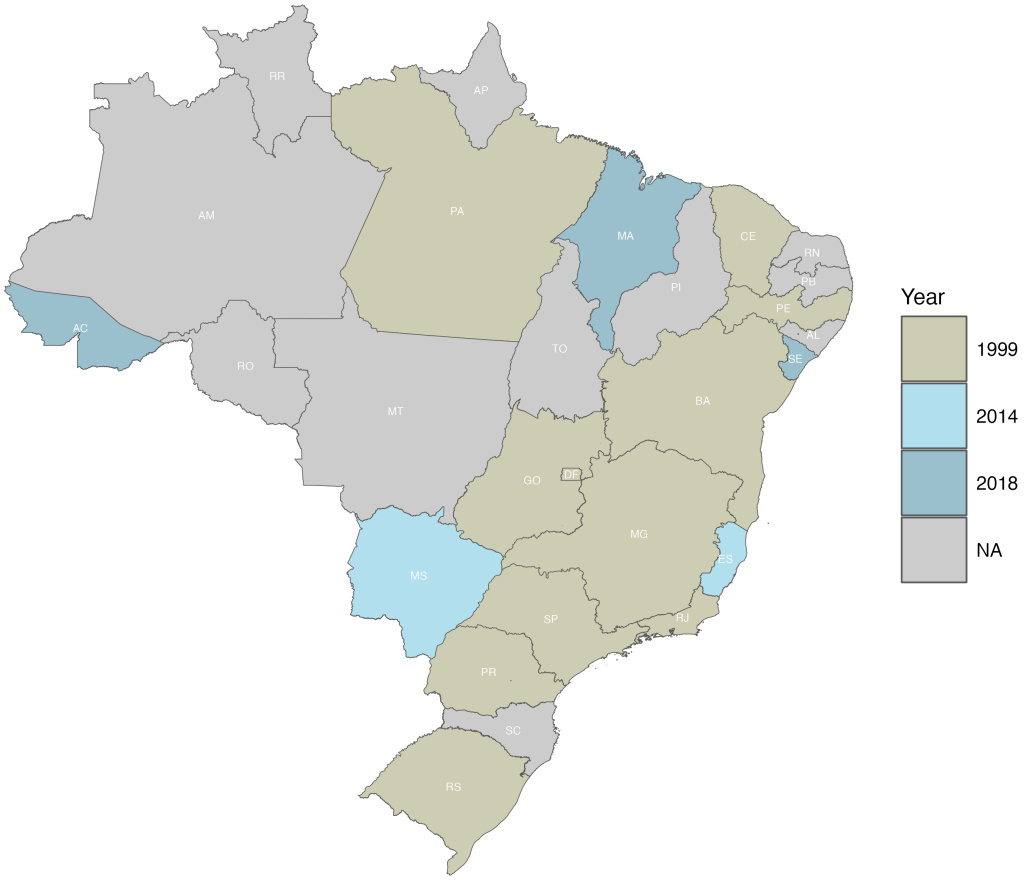

Notes: The figure shows the state boundaries. The legend reads as the year in which the metro area or capital city was introduced in the CPI panel. Many locations were introduced before 1999, so the map reads as 1999 all the cities which were already available in that year. For locations in gold, the CPI coverage started before 1999. For locations in light blue, the coverage started in 2014. For locations in darker blue, the coverage started in 2018. Locations for which CPI data is unavailable are marked in gray.

Table A.4: Locations for which CPI data is available

					Weights (%)		
Location	Type	State	Acronym	Location	Food	LTC Food	HTC Food
Rio Branco	Municipality	Acre	AC	0.5	23.3	12.8	10.4
Belém	Metroarea	Pará	PA	3.9	26.6	15.9	10.7
São Luís	Municipality	Maranhão	MA	3.5	25.5	16.3	9.2
Fortaleza	Metroarea	Ceará	CE	3.2	23.9	13.0	10.9
Recife	Metroarea	Pernambuco	PE	3.9	23.5	11.8	11.6
Aracaju	Municipality	Sergipe	SE	1.0	21.7	10.9	10.8
Salvador	Metroarea	Bahia	BA	6.0	22.4	11.7	10.7
Belo Horizonte	Metroarea	Minas Gerais	MG	9.7	21.7	11.2	10.6
Vitória	Metroarea	Espírito Santo	ES	1.9	17.4	9.3	8.1
Rio de Janeiro	Metroarea	Rio de Janeiro	RJ	9.4	20.2	10.4	9.8
São Paulo	Metroarea	São Paulo	SP	32.3	20.0	9.7	10.3
Curitiba	Metroarea	Paraná	PR	8.1	20.9	11.7	9.2
Porto Alegre	Metroarea	Rio Grande do Sul	RS	8.6	21.1	11.1	10.0
Campo Grande	Metroarea	Mato Grosso do Sul	MS	1.6	21.5	11.9	9.6
Goiânia	Municipality	Goiás	GO	4.2	20.5	11.1	9.4
Brasília	Federal District	Distrito Federal	DF	4.1	16.8	7.1	9.7
Brazil	Country	-	BR	100.0	21.0	10.9	10.1

Notes: The table shows every location we consider in the analysis. The location weights are the officially released figures from the IBGE and were computed from the latest Consumer Expenditure Survey conducted in 2017 and 2018. Location weights come from regional differences in household income. The weights for "Food", LTC Food and HTC Food refers to the data for December 2023. "LTC Food" is "tradable" food, while "HTC Food" is "nontradable" food, according to the latest Central Bank Classification, as exposed in A.4. Occasional rounding errors occur.

A.3.2 Basket of Items Covered in the CPI

Within our sample coverage, the basket of nationally covered sub-items changed three times, so there were baskets that were tracked. These changes happen mainly due to new information available from updated versions of Consumer Expenditure Survey (CES)[26]. The editions of the survey post stabilization of hyperinflation took place in 1995-1996, 2002-2003, 2008-2009 and 2017-2018.

At the beginning of our sample, in 1999, the reference CES was the version conducted in 1995-1996. The CES version 2002-2003 was incorporated into the CPI basket in 2006. The next CES version, 2008-2009, led to a change in the CPI basket in 2012. The latest CES, from 2017-2018, was introduced to the CPI basket in 2020 and was current until the end of our sample.

[26] In Portuguese, Pesquisa de Orçamentos Familiares — POF

A.3.3 Computing the Time Series of Price Changes

Let i be a sub-item (e.g., rice, bus fare, dress), ℓ be a location (e.g., São Paulo, Belo Horizonte, Rio Branco), and t a month. The CPI data provides (i) a monthly weight associated with the sub-item at that location, which we denote by $w_{i,\ell,t}$; and (ii) a monthly percent change in prices, which we denote by $\pi_{i,\ell,t} \equiv \frac{p_{i,\ell,t}}{p_{i,\ell,t-1}} - 1$.

The official data provides the inflation level and the weight for "Food and Beverages" for each date t and location ℓ. Below, we explain how we construct the inflation measures for the baskets of "Non-Food," "Food Tradable", and "Food Nontradable".

Price Changes of an Arbitrary Basket We let the set of all sub-items be denoted by I. Each sub-item is part of exactly one "item" I^k, forming a partition K

$$I \equiv \bigcup_{k \in K} I^k \quad : \quad I^k \bigcap_{k \neq k'} I^{k'} = \{\varnothing\}$$

Let I^k be an item (e.g., fruits, public transportation, women's apparel), which is a set of similar sub-items. Normalize, at the location and monthly level, the weight of each sub-item of I^k so that they sum up to 1. The monthly price change for the item I^k at location ℓ at time t is equal to

$$\pi_{I^k,\ell,t} \equiv \sum_{i \in I^k} \pi_{i,\ell,t} \times \tilde{w}_{i,\ell,t} \equiv \sum_{i \in I^k} \pi_{i,\ell,t} \times \frac{w_{i,\ell,t}}{\sum_{i \in I^k} w_{i,\ell,t}} \tag{4}$$

Let G be a group (e.g., Food and Beverages, Transportation, Apparel), which is a set a set of similar items. Normalize, at the location and monthly level, the weight of each sub-item of I^k so that they sum up to 1. The price change for a group G at location ℓ at time t is equal to

$$\pi_{G,\ell,t} \equiv \sum_{i \in G} \pi_{i,\ell,t} \times \tilde{w}_{i,\ell,t} \equiv \sum_{i \in G} \pi_{i,\ell,t} \times \frac{w_{i,\ell,t}}{\sum_{i \in G} w_{i,\ell,t}} \tag{5}$$

Constructing the Non-Food basket. Let $F_{t,\ell}$ denote the group of items that are classified as "Food". We then compute the inflation level for the basket of "Non-Food" sub-items by construct-

ing a group $NF_{t,\ell}$ as follows. First, we construct the group $NF_{t,\ell}$ as

$$NF_{t,\ell} \equiv \{i \in I : i \notin F_{t,\ell}\} \tag{6}$$

$$\pi_{NF,\ell,t} \equiv \sum_{i \in NF_{\ell,t}} \pi_{i,\ell,t} \times \tilde{w}_{i,\ell,t} \equiv \sum_{i \in NF_{\ell,t}} \pi_{i,\ell,t} \times \frac{w_{i,\ell,t}}{\sum_{i \in NF_{\ell,t}} w_{i,\ell,t}} \tag{7}$$

Constructing the Tradable and Nontradable Food baskets. We borrow from the Brazilian Central Bank a classification of which items are classified as "Tradable" and which ones are Classified as "Non-Tradable", which we use in particular for the group of "Food and Beverages", which we refer generically as "Food"[27] The set of sub-items that are classified as "Food" form a partition of items that are "Tradable" and "Nontradable". Let $TF_{\ell,t}$ be the set of tradable food sub-items at location ℓ and time t. We let $NTF_{\ell,t}$ denote the set of nontradable food sub-items.

$$F_{\ell,t} \equiv TF_{\ell,t} \bigcup NTF_{\ell,t} \quad \text{such that} \quad TF_{\ell,t} \bigcap NTF_{\ell,t} = \{\varnothing\} \tag{8}$$

The inflation of tradable food at location ℓ at date t is given

$$\pi_{TF,\ell,t} \equiv \sum_{i \in TF_{\ell,t}} \pi_{i,\ell,t} \times \tilde{w}_{i,\ell,t} \equiv \sum_{TF_{\ell,t}} \pi_{i,\ell,t} \times \frac{w_{i,\ell,t}}{\sum_{i \in TF_{\ell,t}} w_{i,\ell,t}} \tag{9}$$

while for the nontradable food, we have

$$\pi_{NTF,\ell,t} \equiv \sum_{i \in NTF_{\ell,t}} \pi_{i,\ell,t} \times \tilde{w}_{i,\ell,t} \equiv \sum_{NTF_{\ell,t}} \pi_{i,\ell,t} \times \frac{w_{i,\ell,t}}{\sum_{i \in NTF_{\ell,t}} w_{i,\ell,t}} \tag{10}$$

Computing the Price Level of A Basket. Once we compute the series of inflation for each basket $B \in \{F, NF, TF, NTF\}$, The time series for the price for that basket is computed as

$$p_{B,\ell,t} = p_{B,\ell,0} \prod_{\tau=0}^{t} (1 + \pi_{B,\ell,\tau}) \tag{11}$$

[27] See Appendix A.4 for further detail on such classification.

where we set $p_{B,\ell,0} = 100$ without loss of generality. Applying the natural logs and taking the difference between period $t+h$ and $t-1$, where h stands for the horizon, recovers the dependent variable in the regressions we use throughout the main text.

A.4 Brazilian Central Bank Classification for Goods and Services

Our CPI data come from IBGE. We would like to use a measure of the tradability of goods and services. Since such a classification is not directly available from the IBGE, we rely on the classification developed by the Brazilian Central Bank (BCB).

The BCB uses data on import, export, and production to classify goods and services as "Tradable" and "Nontradable". There is a third category called "Regulated", for sub-items whose prices are controlled by contracts by the competent government (such as bus fare, eletricity fee). These three categories form a partition. Methodological notes with updates to this classification were last posted on Brazilian Central Bank (2019).

We use this classification exclusively for Food goods and services[28]. In such group, there are not "regulated" sub-items, so the goods and services are either classificied as tradable or non-tradable.

Within our sample, there were four versions of the Consumer Expenditure Survey (see, for further details, A.3). For each of these versions, the IBGE defines a national basket of goods and services whose prices will be tracked. The basket of goods actually tracked at each location is a subset of this national basket and depends on regional differences in the consumption habits.

[28] In Portuguese, "Alimentação e Bebidas".

A.5 Matching Crops from IBGE and GAEZ

In this appendix, we list all crops that are matched from the GAEZ dataset and the IBGE crop production data.

Table A.5: Crops matched between GAEZ and the IBGE

Crop Name	GAEZ Acronym	Tradability	Actvitity	Labor Intensity
Banana	bana	HTC	Fruits	149
Barley	barl	LTC	Cereals	82
Beans	bean	HTC	Other seasonal crops	165
Cacao	coco	HTC	Cacao	101
Cassava	casv	HTC	Other seasonal crops	165
Citrus	citr	HTC	Organge	107
Coconut	cocn	HTC	Fruits	149
Coffee	coff	LTC	Coffee	157
Corn	maiz	LTC	Cereals	82
Cotton	cott	LTC	Cotton	14
Cowpea	cowp	HTC	Other seasonal crops	165
Dry peas	dpea	HTC	Vegetables and Legumes	304
Flax fibre	flax	LTC	Oilseeds	169
Groundnut	grnd	LTC	Other seasonal crops	165
Oat	oats	LTC	Cereals	82
Oil palm	oilp	LTC	Other permanent crops	110
Olive	oliv	LTC	Other permanent crops	110
Onion	onio	HTC	Other seasonal crops	165
Rye	ryes	LTC	Cereals	82
Sorghum	bsrg	LTC	Cereals	82
Soybean	soyb	LTC	Soybean	13
Sugar Cane	sugc	LTC	Sugarcane	45
Sunflower	sunf	LTC	Oilseeds	169
Sweet Potato	spot	HTC	Other seasonal crops	165
Tea	teas	LTC	Other permanent crops	110
Tomato	toma	HTC	Vegetables and Legumes	304
Wetland rice	ricw	LTC	Cereals	82
Wheat	whea	LTC	Cereals	82
White Potato	wpot	HTC	Other seasonal crops	165

Notes: Labor intensity is measured as the number of workers per 1,000 hectares, rounded to the nearest whole number. Since labor intensity data is not directly available for each crop, we assign the value from the closest corresponding group whenever necessary. "Activity" is the group defined in the 2017 agricultural census conducted in Brazil. These groups are: "Cereals," "Fruits," "Oilseeds," "Other Seasonal Crops," "Other Permanent Crops," and "Vegetables and Legumes." The "Fruits" category excludes oranges and grapes, while "Oilseeds" excludes soybeans.

These crops correspond to around 90% of total crop production value for the years between 2002 and 2022. The corresponding metric for the share of total land used for crops is even higher, around 95%.

A.6 Construction of μ_ℓ^x and T_ℓ^x

In the main text, we show that the Frechet draws for the productivity imply a link between the State of Technology parameter T_ℓ^x, and the average (or expected) potential productivity, μ_ℓ^x. In the text, this relationship appears in Equation (17), which we reproduce here

$$T_\ell^x = \left[\mu_\ell^x\right]^{\theta^x} \kappa^x$$

In order to recover a measure of average productivity in a way that makes sense in our model, we perform the two adjustments: converting from land to labor productivity and standardizing the units — so we can take an average. The formula to recovering μ_ℓ^x is

$$\mu_\ell^x = \frac{1}{N^x} \sum_\omega Z_\ell^x(\omega) \nu(\omega) p(\omega) \tag{12}$$

where N^x is the number of goods of type x in the Table A.5, $Z_\ell^x(\omega)$ is the productivity of crop ω in location ℓ, measured in Kg/Ha, $\nu(\omega)$ is the input requirement, measured in Wokers/Ha, and $p(\omega)$, is the price in local currency/Kg. The resulting unit is a measure of local currency per worker.

Notice that $\nu(\omega)$ is given by the inverse of labor intensity in Table A.5. This is important since a low input requirement means that the crop is relatively intense in land — soybean is a prominent example. In this case, by construction in equation (12), the relatively more land-intense crops receive a relatively high weight.

Observe that both the input requirement, $\nu(\omega)$, and the price, $p(\omega)$, do not take the index ℓ. Both are based on the national average. The reason is that both conventions are done so that average is sensitive and the final measure corresponds to labor productivity. Using local prices or local input requirements might contaminate the averaging with the connectedness of each location — e.g., the price of a good in a relatively isolated place would be higher, but this would reflect trade costs rather than higher productivity.

Once the measure of μ_ℓ^x, we construct the variable T_ℓ^x. The constant κ^x is absorbed into a normalizing scale: all we need is the relative value of T_ℓ^x to construct $\pi_{j,\ell}^x$, as this variable is homogeneous of degree zero in the vector $[T_\ell^x]$, as shown in Equation (15).

Figure A.3: Measures for the historical μ_ℓ^x for LTC and HTC food goods.

(a) LTC: μ_ℓ^c

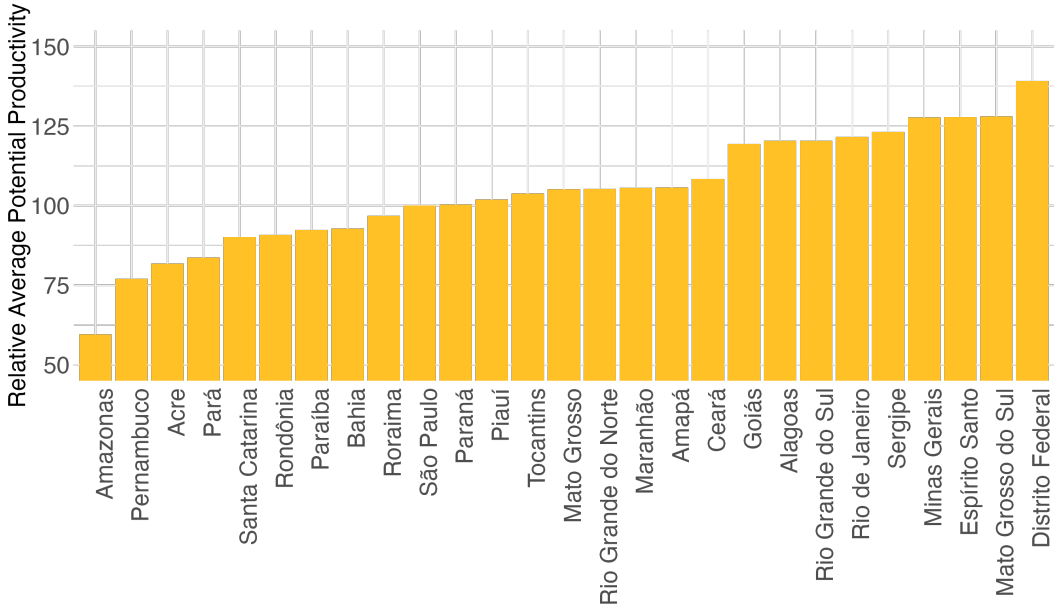

(b) HTC: μ_ℓ^q

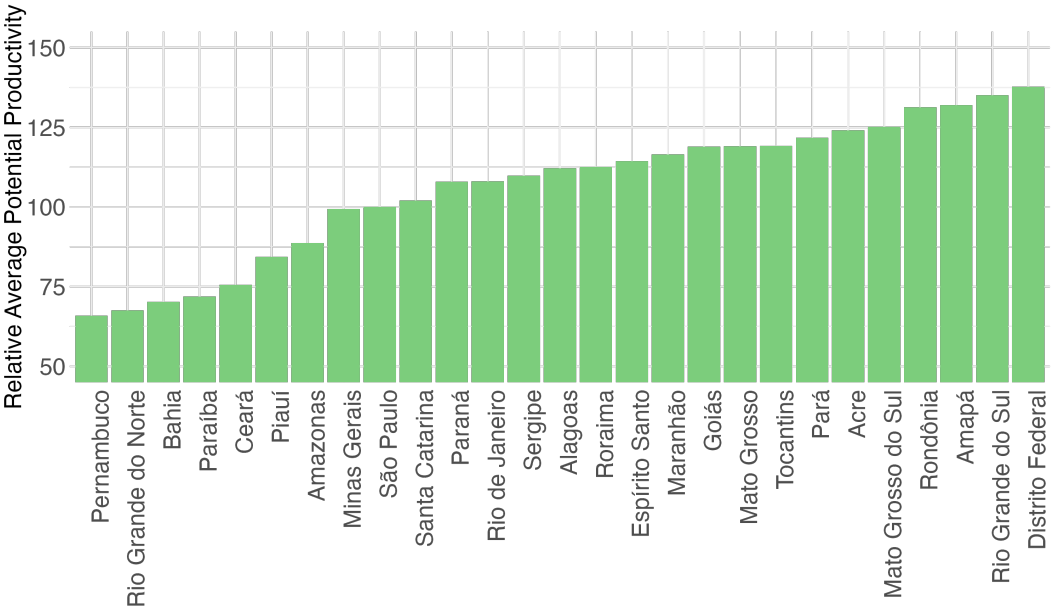

Notes: Panel (a) displays the relative average potential productivity of each state for LTC (low-temperature crop) food goods, while panel (b) shows the corresponding values for HTC (high-temperature crop) food goods. In both panels, productivity levels are expressed relative to the state of São Paulo, which is set to 100 for reference. Each bar represents the productivity value for a given state, with states arranged on the horizontal axis in increasing order from left to right.

Figure A.4: Spatial correlation for μ_ℓ^x for LTC and HTC food goods.

(a) LTC: μ_ℓ^c

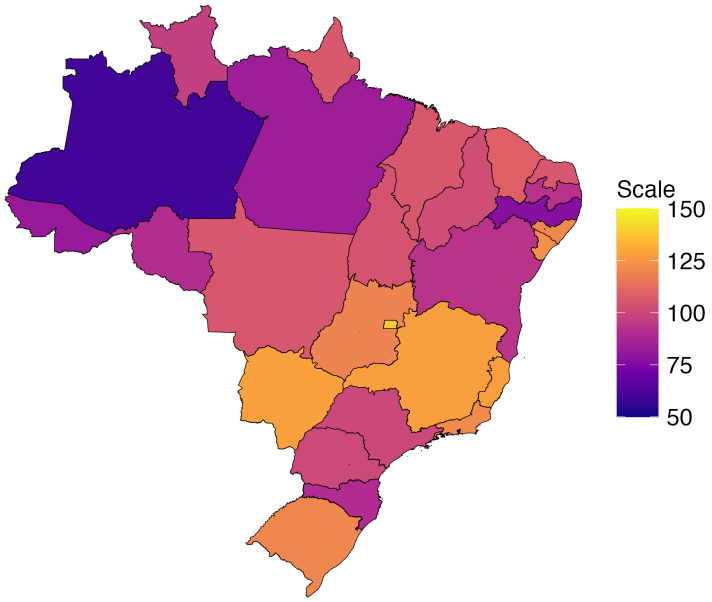

(b) HTC: μ_ℓ^q

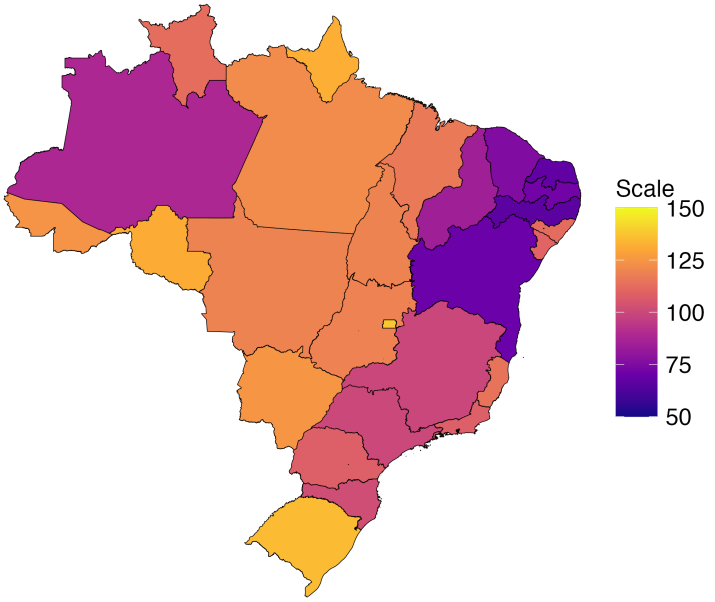

Notes: Panel (a) exhibits the relative average potential productivity of each state for the LTC food goods, while panel (b) exhibits the analogue for the HTC food goods. Both measures are relative to the level of the state of São Paulo, which is normalized to 100. The color scale for each location is comparable.

Results for μ_ℓ^x.

A.7 Construction of the Relative Wages

In the construction of the trade shares, as in Equation 15, we need a measure of the wages costs in each location. For that, we took the average wage for all occupations from Continuous National Household Sample Survey (PNAD Contínua, in Portuguese).

The trade share is homogeneous of degree 0 in the vector of wages. Hence, similar to the case of recovering μ_ℓ^x and T_ℓ^x, we choose one state as a reference and normalize the average wage to the level observed in the State of São Paulo. Since the series started in 2012, we took an average over time, otherwise we would lose more than half of the CPI sample that we use to run the regression Equation 32. The CPI data in our sample starts in 1999.

In the model, $\pi_{j,\ell}^x$ fluctuates because of fluctuations in $\tilde{w}_\ell^x$. Hence, taking the average over time for the relative wage level in each state renders the trade share constant. The resulting average wage is shown below, in figure A.5.

Figure A.5: Relative wage costs

(a) Ordered Wages

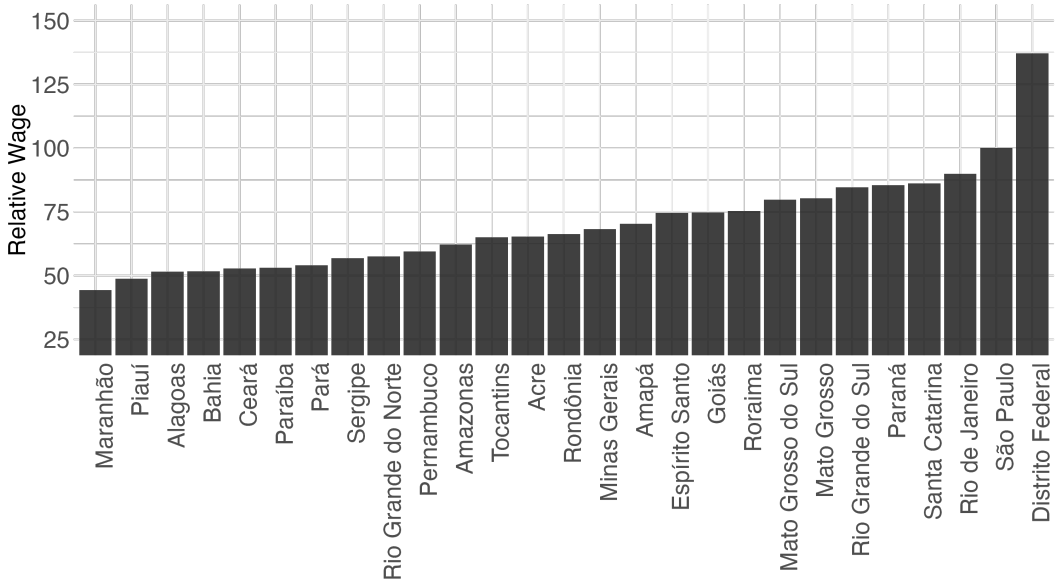

(b) Spatial Dispersion

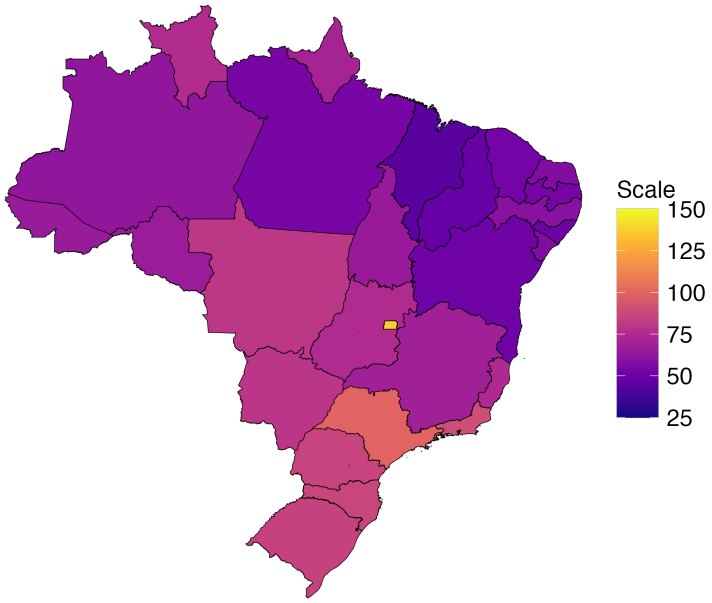

Notes: Panel (a) exhibits the relative wage of each state, ordered from left to right; Panel (b) exhibits the same information in a map, highlighting the spatial dispersion of wages.

A.8 Counterfactual Measures of μ_ℓ^x

Relative to the baseline, the key change in the construction of the counterfactual μ_ℓ^x, denoted by $\mu_\ell^{x\prime}$, is the new draws in $Z_\ell^x(\omega)$, which we denote by $Z_\ell^x(\omega)'$.

Applying the formula in Equation (12), we have the following:

$$\mu_\ell^{x\prime} = \frac{1}{N^x}\sum_\omega Z_\ell^{x\prime}(\omega)\nu(\omega)p(\omega) \tag{13}$$

Letting $g_\ell^x(\omega)$ be the net growth rate of land productivity for variety (x,ω) in location ℓ, we have by construction:

$$Z_\ell^{x\prime}(\omega) = Z_\ell^x(1+g_\ell^x(\omega)) \tag{14}$$

Hence, we can rewrite the rate of change in μ_ℓ^x as

$$\frac{\mu_\ell^{x\prime}-\mu_\ell^x}{\mu_\ell^x} = \sum_\omega \tilde{\mu}_\ell^x(\omega)g_\ell^x(\omega) \tag{15}$$

where

$$\tilde{\mu}_\ell^x \equiv \frac{Z_\ell^x(\omega)\nu(\omega)p(\omega)}{\sum_\omega Z_\ell^x(\omega)\nu(\omega)p(\omega)} \tag{16}$$

gives the of contribution of good ω into μ_ℓ^x. Up to a first-order approximation, provided that $g_\ell^x(\omega)$

$$\begin{aligned}\log(\mu_\ell^{x\prime}) - \log(\mu_\ell^x) &= \log\left(\frac{\mu_\ell^{x\prime}}{\mu_\ell^x}\right)\\ &\approx \frac{\mu_\ell^{x\prime}-\mu_\ell^x}{\mu_\ell^x}\\ &= \sum_\omega \tilde{\mu}_\ell^x(\omega)g_\ell^x(\omega)\end{aligned} \tag{17}$$

Therefore, up to a first-order approximation the proportional change in the average potential productivity can be decomposed into a weighted average of growth rate of each crops' productivity, $g_\ell^x(\omega)$ and the weights are given by the pre-change contributions toward μ_ℓ^x, that is, $\tilde{\mu}_\ell^x(\omega)$.

B Model: Derivations

In this appendix, we provided a detailed derivation of the results for the main model.

B.1 Ideal Price Index

From the nested-CES structure of the utility, the ideal price index for each good type at location $\ell \in \mathcal{L}$

$$P_\ell^c = \left(\int_0^1 p_\ell^c(\omega)^{1-\nu} d\omega \right)^{\frac{1}{1-\nu}} \quad \text{and} \quad P_\ell^q = \left(\int_0^1 p_\ell^q(\omega)^{1-\nu} d\omega \right)^{\frac{1}{1-\nu}}$$

We will use this expressions later on in the derivation.

B.2 Prices

Let the adjusted bundle cost of inputs at location $\ell \in \mathcal{L}$ and good type x be

$$\tilde{w}_\ell^x \equiv \frac{w_\ell}{G^x(s)}$$

The cost of location faced by location j if it were to buy variety ω from location ℓ is given by

$$p_{j,\ell}^x(\omega) = \frac{\tilde{w}_\ell^x}{\tilde{Z}_\ell^x(\omega)} \tau_{j,\ell}^x$$

where $\tau_{j,\ell}^x$ is trade cost of good type x from location ℓ to j and $\tilde{Z}_\ell^x(\omega)$ is the productivity of location ℓ to produce variety ω of good type x, which we label as "EK term" in (24). These EK productivities are independently drawn across locations, varieties, and types from a location-type specific Fréchet Distribution, as in (9):

$$F_\ell^x(\tilde{z}) = e^{-T_\ell^x \tilde{z}^{-\theta^x}}.$$

The probability that location ℓ can supply variety ω of type x to location j at a price at most p is given by

$$\begin{aligned}
G_{j,\ell}^{x}(p) &\equiv \Pr\left\{p_{j,\ell}^{x}(\omega) \leqslant p\right\} \\
&= \Pr\left\{\frac{\tilde{w}_{\ell}^{x}}{\tilde{Z}_{\ell}^{x}(\omega)}\tau_{j,\ell}^{x} \leqslant p\right\} \\
&= \Pr\left\{\frac{\tilde{w}_{\ell}^{x}}{p}\tau_{j,\ell}^{x} \leqslant \tilde{Z}_{\ell}^{x}(\omega)\right\} \\
&= 1 - \Pr\left\{\tilde{Z}_{\ell}^{x}(\omega) \leqslant \frac{\tilde{w}_{\ell}^{x}}{p}\tau_{j,\ell}^{x}\right\} \\
&= 1 - F_{\ell}^{x}\left(\frac{\tilde{w}_{\ell}^{x}}{p}\tau_{j,\ell}^{x}\right) \\
&= 1 - \exp\left\{-T_{\ell}^{x}\left(\tilde{w}_{\ell}^{x}\tau_{j,\ell}^{x}\right)^{-\theta}p^{\theta}\right\}
\end{aligned} \tag{18}$$

Location j buys from the lowest-cost supplier. The probability of location j pays at most p for the type-variety pair (x,ω) is given by

$$\begin{aligned}
G_{j}^{x}(p) &\equiv \Pr\left\{\min_{\ell\in\mathcal{L}} p_{j,\ell}^{x}(\omega) \leqslant p\right\} \\
&= 1 - \Pr\left\{\min_{\ell\in\mathcal{L}} p_{j,\ell}^{x}(\omega) \geqslant p\right\} \\
&= 1 - \Pr\left\{\bigcap_{\ell\in\mathcal{L}}\left(p_{j,\ell}^{x}(\omega) \geqslant p\right)\right\} \\
&= 1 - \prod_{\ell\in\mathcal{L}}\left(1 - G_{j,\ell}^{x}(p)\right)
\end{aligned} \tag{19}$$

Using (18) into (19)

$$\begin{aligned}
G_{j}^{x}(p) &= 1 - \prod_{\ell\in\mathcal{L}}\exp\left\{-T_{\ell}^{x}\left(\tilde{w}_{\ell}^{x}\tau_{j,\ell}^{x}\right)^{-\theta}p^{\theta}\right\} \\
&= 1 - \exp\left\{p^{\theta}\sum_{\ell\in\mathcal{L}} -T_{\ell}^{x}\left(\tilde{w}_{\ell}^{x}\tau_{j,\ell}^{x}\right)^{-\theta}\right\} \\
&= 1 - \exp\left\{-p^{\theta}\Phi_{j}^{x}\right\}
\end{aligned} \tag{20}$$

where

$$\Phi_j^x \equiv \sum_{\ell \in \mathcal{L}} T_\ell^x \left(\tilde{w}_\ell^x \tau_{j,\ell}^x \right)^{-\theta}$$

The ideal price index for location good type x is given by at location j solves

$$\begin{aligned}
\left(P_j^x\right)^{1-\nu} &\equiv \int_0^1 p_\ell^x(\omega)^{1-\nu} d\omega \\
&= \int_0^\infty p^{1-\nu} dG_j^x(p) \\
&= \int_0^\infty p^{1-\nu} \left(\frac{d}{dp} (1 - \exp\left\{ -p^\theta \Phi_j^x \right\} \right) dp \\
&= \int_0^\infty p^{1-\nu} \theta p^{\theta-1} \Phi_j^x \exp\left\{ -p^\theta \Phi_j^x \right\} dp \\
&= \theta \Phi_j^x \int_0^\infty p^{\theta-\nu} \exp\left\{ -p^\theta \Phi_j^x \right\} dp \\
&\equiv \int_0^\infty \left(\frac{y}{\Phi_j^x} \right)^{\frac{1-\nu}{\theta}} \exp\{-y\} dy \\
&= \left(\Phi_j^x\right)^{-\frac{1-\nu}{\theta}} \int_0^\infty y^{\frac{1-\nu}{\theta}} \exp\{-y\} dy \\
&= \left(\Phi_j^x\right)^{-\frac{1-\nu}{\theta}} \Gamma\left(\frac{\theta + 1 - \nu}{\theta} \right) \\
&\equiv \left(\Phi_j^x\right)^{-\frac{1-\nu}{\theta}} \gamma
\end{aligned} \tag{21}$$

where we used, in the sixth row, the change of variable $y \equiv p^\theta \Phi_j^x$, which implies $dy = \theta p^{\theta-1} \Phi_j^x dp$. The Gamma function that appears in the eighth row is given by $\Gamma(t) \equiv \int_0^\infty y^{t-1} \exp\{-y\} dy$, for $t > 1$. We let

$$\gamma \equiv \Gamma\left(\frac{\theta + 1 - \nu}{\theta} \right)$$

The price index P_j^x is then given by

$$\begin{aligned}
P_j^x &= \left(\Phi_j^x\right)^{-\frac{1}{\theta}} \gamma^{\frac{1}{1-\nu}} \\
&\equiv \left(\sum_{\ell \in \mathcal{L}} T_\ell^x \left(\tilde{w}_\ell^x \tau_{j,\ell}^x \right)^{-\theta} \right)^{-\frac{1}{\theta}} \bar{\gamma}
\end{aligned} \tag{22}$$

where we let $\bar{\gamma} \equiv \gamma^{\frac{1}{1-\nu}}$

B.3 Trade Flows

The trade flows expressions are standard expressions in the Eaton and Kortum (2002) framework. Below we show a detailed derivation. There is a continuum of varieties of each type, and the productivity draws are independent across varieties, types and locations. This implies that the probability a location $j \in \mathcal{L}$ buys a variety $\omega \in [0,1]$ of type $x \in \{c,q\}$ is equal to the proportion of goods of this type that location $j \in \mathcal{L}$ will buy from $\ell \in \mathcal{L}$. We denote this *trade share* by $\pi^x_{j,\ell}$.

To find out this share, let us start with the probability that $j \in \mathcal{L}$ buys $\omega \in [0,1]$ from $\ell \in \mathcal{L}$. In what follows, let $\mathcal{L}_{-\ell} \equiv \{j \in \mathcal{L} : j \neq \ell\}$, the set of all locations but ℓ.

$$
\begin{aligned}
\pi^x_{j,\ell} &\equiv \Pr\left\{ p^x_{j,\ell}(\omega) \leqslant \min_{k \in \mathcal{L}_{-\ell}} p^x_{j,k}(\omega) \right\} \\
&= \int_o^\infty \Pr\left\{ \min_{k \in \mathcal{L}_{-\ell}} p^x_{j,k}(\omega) \geqslant p \right\} dG^x_{j,\ell}(p) \\
&= \int_o^\infty \Pr\left\{ \bigcap_{k \in \mathcal{L}_{-\ell}} \left(p^x_{j,k}(\omega) \geqslant p \right) \right\} dG^x_{j,\ell}(p) \\
&= \int_o^\infty \left[\prod_{k \in \mathcal{L}_{-\ell}} \left(1 - G^x_{j,k}(p)\right) \right] dG^x_{j,\ell}(p) \\
&= \int_0^\infty \left[\prod_{k \in \mathcal{L}_{-\ell}} \left(\exp\left\{ -T^x_k \left(\frac{\tilde{w}^x_k \tau_{j,k}}{p} \right)^{-\theta} \right\} \right) \right] dG^x_{j,\ell}(p) \\
&= \int_0^\infty \left[\exp\left\{ p^\theta \sum_{k \in \mathcal{L}_{-\ell}} -T^x_k \left(\tilde{w}^x_k \tau^x_{j,k} \right)^{-\theta} \right\} \right] dG^x_{j,\ell}(p) \\
&= \int_0^\infty \left[\exp\left\{ p^\theta \sum_{k \in \mathcal{L}_{-\ell}} -T^x_k \left(\tilde{w}^x_k \tau^x_{j,k} \right)^{-\theta} \right\} \right] \left(\frac{d}{dp} \left(1 - \exp\left\{ -T^x_\ell \left(\frac{\tilde{w}^x_\ell \tau_{j,\ell}}{p} \right)^{-\theta} \right\} \right) \right) dp
\end{aligned}
$$

Now, using equation (18), we get

$$\begin{aligned}
\pi^x_{j,\ell} &\equiv \int_0^\infty \left[\exp\left\{ p^\theta \sum_{k\in\mathcal{L}_{-\ell}} -T^x_k \left(\tilde{w}^x_k \tau^x_{j,k}\right)^{-\theta} \right\} \right] T^x_\ell \left(\tilde{w}^x_\ell \tau_{j,\ell}\right)^{-\theta} \theta p^{\theta-1} \exp\left\{ -T^x_\ell \left(\tilde{w}^x_\ell \tau_{j,\ell}\right)^{-\theta} p^\theta \right\} dp \\
&= T^x_\ell \left(\tilde{w}^x_\ell \tau_{j,\ell}\right)^{-\theta} \int_0^\infty \theta p^{\theta-1} \exp\left\{ -p^\theta \Phi^x_j \right\} dp \\
&= T^x_\ell \left(\tilde{w}^x_\ell \tau_{j,\ell}\right)^{-\theta} \frac{\Phi^x_j}{\Phi^x_j} \int_0^\infty \theta p^{\theta-1} \exp\left\{ -p^\theta \Phi^x_j \right\} dp \\
&= \frac{T^x_\ell \left(\tilde{w}^x_\ell \tau_{j,\ell}\right)^{-\theta}}{\Phi^x_j} \int_0^\infty \theta p^{\theta-1} \Phi^x_j \exp\left\{ -p^\theta \Phi^x_j \right\} dp \\
&= \frac{T^x_\ell \left(\tilde{w}^x_\ell \tau_{j,\ell}\right)^{-\theta}}{\Phi^x_j} \left[-\exp\left\{ -p^\theta \Phi^x_j \right\} \right]_{p=0}^\infty \\
&= \frac{T^x_\ell \left(\tilde{w}^x_\ell \tau_{j,\ell}\right)^{-\theta}}{\Phi^x_j}
\end{aligned} \tag{23}$$

B.4 Indirect Utility

Under the assumption of the Stone-Geary utility function, the indirect utility is given by

$$\mathcal{U}(c^o_{i,j}, c^f_{i,j}) = (1-\alpha^f)\log(c^o_{i,j}) + \alpha^f \log(c^f_{i,j} - \underline{c}^f) \tag{24}$$

The outside good is a numeraire, the price of food is P^f_j and the income is $y_{i,j}$. Thus, the demand for each good is

$$\mathcal{C}^o_{i,j} = (1-\alpha^f)(y_{i,j} - \underline{c}^f P^f_j) \tag{25}$$

$$\mathcal{C}^f_{i,j} = \underline{c}^f + \alpha^f \frac{(y_{i,j} - \underline{c}^f P^f_j)}{P^f_j} \tag{26}$$

Hence, the food expenditure share is given by

$$s^f_{i,j} \equiv \frac{\mathcal{C}^f_{i,j} P^f_j}{y_{i,j}} = \alpha^f + (1-\alpha^f)\psi^f_{i,j} \tag{27}$$

where $\psi_{i,j}^f$ is the subsistence ratio, the share of income that is needed to pay for the minimum food consumption:

$$\psi_{i,j}^f \equiv \frac{\underline{c}^f P_j^f}{y_{i,j}} \tag{28}$$

Plugging the demand for each good into the utility, we recover the indirect utility function:

$$\mathcal{V}_{i,j} \equiv V(y_{i,j}, P_j^f) = \underbrace{(1-\alpha^f)\log(1-\alpha^f) + \alpha^f \log(\alpha^f)}_{\equiv \tilde{\alpha}} + \log(y_{i,j} - \underline{c}^f P_j^f) - \alpha^f \log(P_j^f) \tag{29}$$

We write

$$\mathcal{V}_{i,j} = \tilde{\alpha} + \log(y_{i,j} - \underline{c}^f P_j^f) - \alpha^f \log(P_j^f) \tag{30}$$

B.4.1 Effect of Increasing Food Prices

The derivative of the indirect function with respect to the food prices is given by

$$\begin{aligned}
\frac{\partial \mathcal{V}_{i,j}}{\partial P_j^f} &= \frac{-\underline{c}^f}{y_{i,j} - \underline{c}^f P_j^f} - \alpha^f \frac{1}{P_j^f} \\
&= \frac{-\underline{c}^f}{y_{i,j} - \underline{c}^f P_j^f} \frac{P_j^f}{P_j^f} - \alpha^f \frac{1}{P_j^f} \\
&= -\frac{1}{P_j^f} \left(\frac{\underline{c}^f P_j^f}{y_{i,j} - \underline{c}^f P_j^f} + \alpha^f \right) \\
&= -\frac{1}{P_j^f} \left(\frac{\psi_{i,j}^f y_{i,j}}{y_{i,j} - \psi_{i,j}^f y_{i,j}} + \alpha^f \right) \\
&= -\frac{1}{P_j^f} \left(\frac{\psi_{i,j}^f}{1 - \psi_{i,j}^f} + \alpha^f \right) \\
&= -\frac{1}{P_j^f} \left(\frac{\alpha^f + \psi_{i,j}^f (1-\alpha^f)}{1 - \psi_{i,j}^f} \right)
\end{aligned}$$

This derivative is more negative: increasing food prices decreases the indirect utility ceteris paribus. This derivative also gets more negative as $\psi^f_{i,j}$ increases.

B.4.2 Exact Income Compensation

Suppose that the price of food change proportionally by a factor g:

$$P_j^{f\prime} = P_j^f(1+g) \tag{31}$$

The goal of this section is to derive by which factor income $e_{i,j}$ needs to change to achieve the same level of utility, at the initial prices. That is, $e_{i,j}$ that solves the following equation:

$$V(y_{i,j}(1+e_{i,j}), P_j^f) = V(y_{i,j}, P_j^f(1+g)) \tag{32}$$

The equality requires

$$\log(y_{i,j}(1+e_{i,j}) - \underline{c}^f P_j^f) - \alpha^f \log(P_j^f) = \log(y_{i,j} - \underline{c}^f P_j^f(1+g)) - \alpha^f \log(P_j^f(1+g)) \tag{33}$$

Now, using the fact that

$$\underline{c}^f P_j^f = \psi^f_{i,j} y_{i,j} \tag{34}$$

and that

$$\underline{c}^f P_j^{f\prime} = \underline{c}^f P_j^f(1+g) \tag{35}$$

$$= \psi^f_{i,j} y_{i,j}(1+g) \tag{36}$$

we have that

$$\log(y_{i,j}(1+e_{i,j}) - \psi^f_{i,j} y_{i,j}) - \alpha^f \log(P_j^f) = \log(y_{i,j} - \psi^f_{i,j} y_{i,j}(1+g)) - \alpha^f \log(P_j^f(1+g)) \tag{37}$$

implying

$$(y_{i,j}(1+e_{i,j}) - \psi^f_{i,j} y_{i,j}) = (y_{i,j} - \psi^f_{i,j} y_{i,j}(1+g))(1+g)^{-\alpha^f} \tag{38}$$

or

$$(1+e_{i,j}) - \psi^f_{i,j} = (1-\psi^f_{i,j}(1+g))(1+g)^{-\alpha^f} \tag{39}$$

or

$$e_{i,j} = \psi^f_{i,j} + (1-\psi^f_{i,j}(1+g))(1+g)^{-\alpha^f} - 1 \tag{40}$$

or

$$e_{i,j} = \psi^f_{i,j} + ((1+g)^{-\alpha^f} - 1) - \psi^f_{i,j}(1+g)^{1-\alpha^f} \tag{41}$$

so let us write

$$\mathcal{E}_{i,j}(\psi^f_{i,j}, g) \equiv e_{i,j} = \psi^f_{i,j} + ((1+g)^{-\alpha^f} - 1) - \psi^f_{i,j}(1+g)^{1-\alpha^f} \tag{42}$$

Some properties of this function $\mathcal{E}_{i,j}$ are

a) $\mathcal{E}_{i,j}(\psi^f_{i,j}, 0) = 0$

b) Decreasing in g

c) Decreasing in $\psi^f_{i,j}$ if $g > 0$, and increasing in $\psi^f_{i,j}$ if $g < 0$

d) Convex in g

Property (a) follows by construction.

For Property (b), observe that

$$\frac{\partial \mathcal{E}_{i,j}}{\partial g} = -\alpha^f (1+g)^{-\alpha-1} - \psi^f_{i,j}(1-\alpha)(1+g)^{-\alpha^f} < 0 \tag{43}$$

Property (a) + (b) imply that households would be willing to pay not to face higher prices. This is rather mechanical: the indirect utility is increasing in income and decreasing in prices.

For property (c), observe that

$$\frac{\partial \mathcal{E}_{i,j}}{\partial \psi^f_{i,j}} = 1 - (1+g)^{1-\alpha^f} \tag{44}$$

When $g = 0$, this derivative evaluates as 0. Now, using the fact that

$$\frac{\partial \mathcal{E}_{i,j}}{\partial g}\frac{\partial \mathcal{E}_{i,j}}{\partial \psi^f_{i,j}} = -(1-\alpha^f)(1+g)^{-\alpha^f} < 0 \tag{45}$$

we see that $\mathcal{E}_{i,j}$ is increasing in $\psi^f_{i,j}$ if g is negative and decreasing in g if positive.

Finally, for property (d), observe that the second derivative of $\mathcal{E}_{i,j}$ with respect to g is positive:

$$\frac{\partial^2 \mathcal{E}_{i,j}}{\partial g^2} = \alpha^f(1-\alpha^f)(1+g)^{-\alpha-1}\left[(1+g)^{-1} + \psi^f_{i,j}\right] > 0 \tag{46}$$

B.4.3 Exact Growth Rate in Food Prices

Owing to the Cobb-Douglas structure of the composite for the two goods, the price of the food basket is given by

$$P^f_\ell = \left(\frac{P^c_\ell}{\alpha^c}\right)^{\alpha^c}\left(\frac{P^q_\ell}{\alpha^q}\right)^{\alpha^q} \tag{47}$$

Let g be the (net) growth rate of price of food, g^c and g^q their analogue for the LTC and the HTC. Hence, the final price is given by

$$P^f_\ell(1+g) = \left(\frac{P^c_\ell(1+g^c)}{\alpha^c}\right)^{\alpha^c}\left(\frac{P^q_\ell(1+g^q)}{\alpha^q}\right)^{\alpha^q} \tag{48}$$

or

$$P^f_\ell(1+g) = \left(\frac{P^c_\ell}{\alpha^c}\right)^{\alpha^c}(1+g^c)^{\alpha^c}\left(\frac{P^q_\ell}{\alpha^q}\right)^{\alpha^q}(1+g^q)^{\alpha^q} \tag{49}$$

or

$$(1+g) = (1+g^c)^{\alpha^c}(1+g^q)^{\alpha^q} \tag{50}$$

Using a log approximation, the growth rate g can be written as a weighted average of the changes g^c and g^q

$$g \approx \alpha^c g^c + \alpha^q g^q \tag{51}$$

The approximation is good with the growth rates (g^c, g^q) are small, but performance deteriorates for large changes - positive or negative. In our results, the changes in prices are large. The under-

lying reason is that the changes in potential productivity, captured by μ_ℓ^x are substantial.